Geochemical and petrographic analyses of new petroleum source rocks from the onshore Upper Jurassic and Lower Cretaceous of Lebanon

Layla El Hajj, François Baudin, Ralf Littke, Fadi H. Nader, Raymond Gèze, Sibelle Maksoud, Dany Azar

▶ **To cite this version:**

Layla El Hajj, François Baudin, Ralf Littke, Fadi H. Nader, Raymond Gèze, et al.. Geochemical and petrographic analyses of new petroleum source rocks from the onshore Upper Jurassic and Lower Cretaceous of Lebanon. International Journal of Coal Geology, 2019, 204, pp.70-84. 10.1016/j.coal.2019.02.003 . hal-02128184

HAL Id: hal-02128184
https://hal.science/hal-02128184

Submitted on 21 Oct 2019

HAL is a multi-disciplinary open access archive for the deposit and dissemination of scientific research documents, whether they are published or not. The documents may come from teaching and research institutions in France or abroad, or from public or private research centers.

L'archive ouverte pluridisciplinaire **HAL**, est destinée au dépôt et à la diffusion de documents scientifiques de niveau recherche, publiés ou non, émanant des établissements d'enseignement et de recherche français ou étrangers, des laboratoires publics ou privés.

Accepted Manuscript

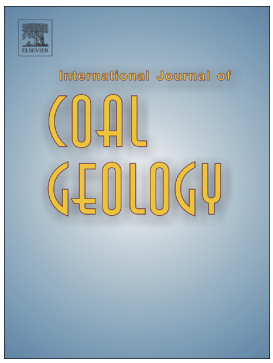

Geochemical and petrographic analyses of new petroleum source rocks from the onshore Upper Jurassic and Lower Cretaceous of Lebanon

Layla el Hajj, François Baudin, Ralf Littke, Fadi H. Nader, Raymond Geze, Sibelle Maksoud, Dany Azar

PII: S0166-5162(18)31129-7
DOI: https://doi.org/10.1016/j.coal.2019.02.003
Reference: COGEL 3156

To appear in: *International Journal of Coal Geology*

Received date: 17 December 2018
Revised date: 13 February 2019
Accepted date: 14 February 2019

Please cite this article as: L.e. Hajj, F. Baudin, R. Littke, et al., Geochemical and petrographic analyses of new petroleum source rocks from the onshore Upper Jurassic and Lower Cretaceous of Lebanon, International Journal of Coal Geology, https://doi.org/10.1016/j.coal.2019.02.003

This is a PDF file of an unedited manuscript that has been accepted for publication. As a service to our customers we are providing this early version of the manuscript. The manuscript will undergo copyediting, typesetting, and review of the resulting proof before it is published in its final form. Please note that during the production process errors may be discovered which could affect the content, and all legal disclaimers that apply to the journal pertain.

ACCEPTED MANUSCRIPT

Geochemical and petrographic analyses of new petroleum source rocks from the onshore Upper Jurassic and Lower Cretaceous of Lebanon

Layla EL HAJJ[1,2,*] Layla.el_hajj@sorbonne-universite.fr, François BAUDIN[2], Ralf LITTKE[3], Fadi H. NADER[4], Raymond GEZE[1], Sibelle MAKSOUD[1,5], Dany AZAR[1]

[1]Lebanese University, Faculty of Sciences II, Fanar-Maten, P.O.box 26110217, Lebanon

[2]Sorbonne Université, CNRS, UMR 7193 Institut des Sciences de la Terre de Paris (ISTeP), 4 place Jussieu, 75005 Paris, France

[3]Energy & Mineral Resources Group (EMR), Institute of Geology and Geochemistry of Petroleum and Coal, RWTH Aachen University, Lochnerstrasse 4-20, 52056 Aachen, Germany

[4]Geosciences Division, IFP Energies nouvelles, 1&4 Avenue de Bois-Préau, 92852 Rueil-Malmaison Cedex, France

[5]State Key Laboratory of Palaeobiology and Stratigraphy, Nanjing Institute of Geology and Palaeontology, Chinese Academy of Sciences, Nanjing 210008, People's Republic of China

[*]Corresponding author.

Abstract

The recent interest in the Lebanese petroleum potential led to new studies mainly concerning marine petroleum source rocks, without taking in consideration the dysodiles and other associated facies from the Upper Jurassic and the Lower Cretaceous. These organic-rich outcrops of metric thickness (max. 3 m) are of limited lateral extension and often found next to volcanic deposits. Sixty-three samples were collected from 25 different localities, and were subdivided into three facies that are presented in this paper: (i) dysodiles formed by the

ACCEPTED MANUSCRIPT

superposition of millimetric layers that are easy to separate; (ii) dysodiles-like with distinct, but more compacted layers; (iii) non-dysodiles where the layering is not visible. The aim of this work is to assess the origin of these organic-rich rocks, and to evaluate their source rock potential. We used herein Rock-Eval pyrolysis, elemental analysis, palynofacies observation, organic petrography and molecular geochemical analyses. Rock-Eval pyrolysis reveals a very good to excellent source-rock potential for all above cited rock types, with average total organic carbon (TOC) of 14 ± 7% for the dysodiles, 19 ± 12% for the dysodiles-like and 13 ± 9% for the non-dysodiles. Hydrogen index (HI) and oxygen index (OI) values indicate a type I to II kerogen for the dysodiles (average HI= 649 ± 162 mg HC/g TOC), type I to II kerogen for the dysodiles-like (average HI= 340 ±182 mg HC/g TOC) and type III kerogen for the non-dysodiles (average HI= 145 ± 42 mg HC/g TOC). The dominance of fluorescent amorphous organic matter (AOM) and alginite macerals confirm an algal/bacterial source of organic matter for the dysodiles. The presence of opaque AOM, phytoclasts, sporinites and cutinites macerals, suggests a variable terrestrial organic matter input for the dysodiles-like and non-dysodiles. Maturity parameters such as Tmax values (on average 428 ±7 ˚C for dysodiles, 429 ±6 ˚C for dysodiles-like and 424 ±10 ˚C for non-dysodiles), vitrinite reflectance (<0.5%) and Carbon Preference Index (>1) indicate that the organic matter is still thermally immature. The present study sheds light on the long forgotten dysodile shales and similar material, and their importance as potential source rocks or oil shales. A comparison with local and regional source rocks is provided in order to emphasize the specific character of the dysodile deposits.

Key words Dysodiles, kerogen type, source rocks, immature, Rock-Eval, palynofacies, petrography.

ACCEPTED MANUSCRIPT

1. Introduction

The position of the Levant Basin in the eastern Mediterranean region at the intersection of the Arabian, African and Eurasian plates invokes its geological complexity. The resulted scientific curiosity together with the discovery of several oil and gas fields has attracted the attention of academic scholars and industry experts for a long time (Dubertret, 1934). In Lebanon (onshore), scientific research was accompanied by previous hydrocarbon exploration attempts. The seven exploration wells drilled between 1947 and 1967 in onshore Lebanon were not successful, yielding no commercial volumes of oil or gas (Nader, 2011). Recently, important new gas field discoveries have been made in the Levant Basin (Tamar, Leviathan, Aphrodite, Zohr and Calypso), boosting the interest in the Lebanese hydrocarbon potential and petroleum systems (Nader, 2011; 2014a). Bou Daher *et al*. (2016) studied in great detail different potential source rocks from onshore Lebanon collected from outcrops and shallow boreholes. The age of these samples, ranges between the Kimmeridgian and the late Paleocene. Their results proved that the Paleocene accommodates oil-prone and gas-prone source-rocks, belonging to kerogen type II and III (TOC = 0.8%). They also showed that the Campanian – Lower Maastrichtian marly limestones from the South of Lebanon (TOC = 5.4%) (Bou Daher *et al*., 2015), the Upper Santonian – Upper Campanian fine-grained carbonates and marls from the North of Lebanon (TOC = 2.4%) (Bou Daher *et al*., 2014), and the Cenomanian marine carbonates (TOC = 1.1%) (Bou Daher *et al*., 2016) have very good source rock potential containing oil-prone type II and type IIS kerogens. According to their work, the Albian source rocks contain a type III/IV kerogen and have low TOC values (0.5%) making them poor-quality petroleum source rocks. In contrast, the studied Neocomian coaly shales (TOC = 17.9%) and the Kimmeridgian shales (TOC = 53.3%) contain type III kerogen, often in great quantity (Bou Daher *et al*., 2016). Assumptions are made on the offshore source rocks, which might include Oligocene –

ACCEPTED MANUSCRIPT

Miocene siliciclastics, kerogen type IIS-bearing Senonian marls and chalks (TOC = 10%), type II-bearing mid-Jurassic limestones (TOC = 2.6%), and Triassic and Lower Jurassic organic-rich layers (TOC = 0.5 – 1.4%) (Bou Daher *et al*., 2016), as well as Silurian shales (Feinstein *et al*., 2002).

However, several laterally less extensive, lacustrine shales, well present at outcrops in Lebanon, were not included in these previous studies. Such lacustrine shales might act as oil shales or petroleum source rocks, the dysodile shales and other associated facies that we will characterize and discuss in the present contribution. According to the description by Cordier (1808), dysodiles shales are organic-rich rocks formed by the superposition of millimetric layers that are easy to separate. Old citations mentioned their presence in the Lower Cretaceous sandstones of Mount Lebanon (Botta, 1831), in the South of Lebanon (Fraas, 1878) and in the center of Lebanon (Janensch, 1925).

Recent fieldwork focuses on many dysodile deposits and associated facies belonging to different geological units and ages within the Kimmeridgian and Lower Cretaceous from North to South of Lebanon. To date, the depositional environment of these organic-rich deposits and their importance as a potential petroleum source rock remain largely unknown. Thus, the major objectives of this study are to assess the origin of the organic-rich deposits and the enclosed kerogen, and to evaluate their source rock potential.

2. Geological setting

Lebanon is located on the eastern margin of the Levant basin, in the north-western part of the Arabian platform (fig.1). Two main mountains form the country, Mount Lebanon to the West and Mount Anti-Lebanon to the East, separated by the Bekaa valley. Lebanon is subdivided by many major faults oriented NNE-SSW, part of the Levant Fracture system (Nader, 2011).

ACCEPTED MANUSCRIPT

The stratigraphic column of Lebanon (fig.2) is dominated by carbonates deposited under marine conditions. The oldest known deposits date back to the early Jurassic (Nader, 2014b). The pre-Jurassic deposits are not exposed onshore Lebanon.

Rarely mentioned in the bibliography, the dysodiles and associated facies, crop out in small isolated basins (max. lateral extension 1 km, max. thickness 3 m), in the Upper Jurassic (Kimmeridgian) and the Lower Cretaceous formations (Lower Barremian and Albian). A different paleoenvironment characterizes each formation. Therefore, the Upper Jurassic corresponds to a shallow marine environment, represented by 1300 m of dolomitized carbonates, followed by 180 m of volcanic deposits, marls and carbonates of Kimmeridgian age (Noujaim Clark and Boudagher-Fadel, 2001; Nader, 2014b). The Lower Barremian (Granier *et al*, 2016) is mainly fluvio-deltaic and lacustrine, characterized by variable thickness (0 to 300 m) of sandstone, laminated claystone and lacustrine carbonates rich in charophytes (Granier *et al*., 2015), while the Albian is a margino-littoral environment consisting of carbonates and claystones. During the Upper Jurassic and the Lower Cretaceous, Lebanon was in a local extension phase (fig.2) leading to volcanic activity associated to block faulting and fault reactivation (Brew *et al*., 2001). It is known that these tectonic instabilities could be the cause of various small lacustrine basins favorable for the accumulation and preservation of the organic matter (Kelts, 1988). Moreover, the proximity to the volcanic deposits, lets us speculate on a close relation between volcanic activity and the deposition of these organic-rich facies. Lava flows could have formed small basins where water was retained and life existed in bacterial mats, whereas preservation was controlled by magmatic intoxications and thus a lack of microbial degradation (Veltz, 2008). Furthermore, the fluvio-deltaic setting during the Lower Barremian could have enriched these small lakes in sediments and nutrients leading to a higher productivity. Additionally, the tropical position of Lebanon during the Upper Jurassic – Lower Cretaceous period, favors the continuous

ACCEPTED MANUSCRIPT

lacustrine primary productivity throughout the year (Talbot and Allen, 1996). Besides, the rapid burial of the organic matter in a lacustrine environment (Bohacs *et al*., 2000), and the anoxic bottom conditions in small isolated lakes (Zimmerle, 1985), may have enhanced the organic matter preservation, and the formation of these organic-rich deposits.

3. Material

Sixty-three samples were collected from 25 different outcrop localities, located from North to South of Lebanon (fig.1 and table 1), including 35 dysodiles, 13 dysodiles-like (more compact than 'true' dysodiles) and 15 non-dysodiles (non-laminated massive organic-rich rocks) (fig. 3).

4. Methods

The collected samples were studied by geochemical and optical methods, some of them applied to all samples and others to selected samples, covering a wide range of age and of geochemical characteristics of the bulk rocks (Table 2).

4.1. Rock-Eval pyrolysis

Rock-Eval pyrolysis allows the characterization of the organic matter, and gives detailed information on the hydrocarbon generation potential, kerogen type and thermal maturation degree (Espitalié *et al*., 1985; Behar *et al*., 2001). All samples (63) were analyzed by the Rock-Eval pyrolysis, using the *Rock-Eval VI* instrument, *Turbo version (Vinci Technologies)* of the ISTeP laboratory (Sorbonne Université, Paris, France). For the Rock-Eval pyrolysis, up to 60 mg of the lighter less organic-rich samples, and 15 mg of the darker, more organic-rich samples, were used. The analyzed sequence consists of two replicas of each sample and a standard after each 10 analyses. The results were similar for the replicas. The pyrograms were constantly checked in order to detect any problem and prevent the saturation of the FID detector and erroneous results (Carvajal-Ortiz and Gentzis, 2015).

ACCEPTED MANUSCRIPT

This analysis provides the following parameters: S1, S2, S3, TOC, MinC and Tmax. These parameters permit the calculation of Hydrogen index (HI) = S2/TOC*100 (mg HC/g TOC); Oxygen index (OI) = S3/TOC*100 (mg CO_2/g TOC) and petroleum potential (PP) = S1+S2 (mg HC/ g rock) (Behar *et al.*, 2001). To characterize the kerogen type, the hydrogen index (HI) and the oxygen index (OI) are plotted in a pseudo Van Krevelen diagram.

4.2. Elemental analysis

This analysis measures the concentration of N, C, H, S and O within the organic matter. We proceeded herein, using the isolation of the organic matter method described by Durand & Nicaise (1980). The fragmented rocks are first digested by the hydrochloric acid (HCl, 33%) in order to eliminate the carbonates, then by the hydrofluoric acid (HF, 70%) in order to eliminate the silicates, and finally with boiling HCl to eliminate all the neo-formed minerals (notably the fluorosilicates). After each acid digestion, the pH was neutralized by washing the sample with demineralized water. In all, the organic matter was isolated from 26 samples.

Two mg of each sample were analyzed in the ISTeP laboratory (Sorbonne Université, Paris, France) using the elemental analyzer CHNS-O Flash 2000 from ThermoFischer.

According to Behar *et al*. (2001), the errors of these measurements are 0.5% for C, 0.7% for H, 1% for N, 3.05% for O and 1% for S. The sum of all of the percentages may not be equal to 100% due to the presence of some residual minerals non-detectable by this method (Durand and Monin, 1980; Vandenbroucke and Largeau, 2007). Using these concentrations, the van Krevelen diagram (atomic H/C vs O/C) was applied in order to evaluate the origin of the organic matter and its maturation level.

4.3. Palynofacies analysis

Palynofacies analysis is a semi-quantitative method used in order to visualize the microscopic components of the organic matter, and so determine its origin (Combaz, 1980; Tyson, 1995).

ACCEPTED MANUSCRIPT

The palynofacies analysis was performed on the same 26 samples used for the elemental analysis. Slides from the isolated organic matter (crude and filtered to 10µm) were prepared using polyvinyl alcohol and UV resin (NOA61). A Zeiss optical microscope coupled with UV light served for the observation and counting of the organic matter components. The counting was done through a grid implanted in the oculars, and for each sample, 450 to 850 surface units were counted.

According to the classification done by Tyson (1995), the identifiable organic matter components are:

- Amorphous organic matter (AOM) deriving from phytoplanktonic blooms, fecal pellets of zooplankton and bacterial mats of laminated or unidentifiable structure.
- Phytoclasts deriving from ligno-cellulosic plant debris. These phytoclasts lose their initial structure and become opaque due to many factors such as the thermal maturation, oxidation and remineralization. In this way, we can distinguish between PM4 being the most opaque phytoclasts, PM1 and PM2 that are less opaque and still preserve some of their initial structure, and PM3 that are the lightest and are mostly leave cuticles.
- Palynomorphs containing sporomorphs (spores and pollen grains), the organic parts of phytoplankton and macro-algae (dinoflagellate cysts, Botryococcus, etc.) and zoomorphs (basal linings of foraminifera, Chitinozoa, scolecodonts, insects).

4.4. Organic petrography

This method allows the identification of the macerals forming the organic matter and provides information on the thermal maturation of the rock. Thirty-two polished sections were prepared at RWTH Aachen by embedding cuttings in a 10:3 mixture of epoxy resin (*Araldite® XW396*) and hardener (*Araldite® XW397*), and then drying them at 37 °C for 12

ACCEPTED MANUSCRIPT

h. The cutting and polishing of the samples followed exactly the procedure described by Sachse *et al*. (2012). Random vitrinite reflectance (VRr) was measured by counting 100 points/sample, at a magnification of 500x in a dark room with a *Zeiss Axio Imager* microscope equipped with an incident white light tungsten-halogen lamp (12V, 100W), an *Epiplan-NEOFLUAR* 50x/0.85 oil immersion objective, and using *Zeiss* immersion oil with a refraction index of 1.518. A leuco-saphire mineral standard (0.592%) served for the calibration, while the software *DISKUS Fossil*, v.460.810 (*Technisches Büro Carl H. Hilgers*, Königswinter, Germany) was used to process the data.

Maceral analysis was also performed on all 32 samples using incident white light, and ultraviolet light (280-380 nm). The revised ICCP maceral groups' classification served for the macerals identification.

4.5. Molecular geochemistry

Molecular geochemistry helps identifying the molecular compounds found in the solvent soluble organic matter, and therefore gives an idea on its' origin and on the depositional environment. Twenty-one samples underwent the molecular analysis at RWTH Aachen University, Germany.

Using a DIONEX ASE 150 instrument (Thermo Scientific), 4 grams of bulk rock powder were extracted by using 40 ml of dichloromethane (DCM), in a high-pressure cell at 100°C and 100 bar for 14 minutes. The fractioning of the extracts was done using silica gel liquid chromatography into 4 fractions: the aliphatic fraction F1 was eluted by 5 ml of pentane; the aromatic fractions F2 and F3 were obtained using 5 ml of pentane/DCM (40:60) and 5 ml DCM, respectively, while the NSO compound fraction F4 was eluted by 5 ml of methanol.

ACCEPTED MANUSCRIPT

4.5.1. GC-FID

The composition of the aliphatic fractions was investigated using a *Carlo Ebra Strumentazione HRGC 5300* gas chromatograph (GC) equipped with a flame ionization detector (FID). The initial temperature, set for 3 min, was 60 °C, and then increased by 5 °C/min to reach 310 °C. This final temperature was held for 20 min. A splitless mode injection was set to 60 s. A 30 m long *Zebron ZB-1* capillary column served for the compounds separation, using hydrogen as carrier gas. The chromatograms were interpreted using the *Atlas CDS* software.

5. Results

5.1. Rock-Eval pyrolysis

Table 3 shows the Rock-Eval pyrolysis results according to the three studied facies: dysodiles, dysodiles-like and non-dysodiles. A boxplot (fig.4) helped identifying the outliers, the values of which were not considered for the calculation of the average, in order to have a more significant mean for each rock type.

For the dysodile samples, S1 values vary between 0.12 and 13.18 mg HC/g rock (average 2.40 ±3.39 mg HC/g rock), S2 values between 6.28 and 219.44 mg HC/g rock (average 99.67 ± 62.26 mg HC/g rock) and S3 values between 0.44 and 10.79 mg CO_2/g rock (average 3.76 ± 2.60 mg CO_2/g rock). TOC is between 1.42 and 24.89% (average 14.44 ± 7.10%), while TIC varies between 0.07 and 8.45% (average 2.40 ±2.28%) with the exception of one having 9.85% TIC. Moreover, Tmax shows values between 417 and 440 ˚C (average 428 ±7 ˚C). Table 3 also gives the calculated indexes HI, OI and PP. The hydrogen index varies between 302 and 915 mg HC/g TOC (average 649 ± 162 mg HC/g TOC), the oxygen index between 7 and 84 mg CO_2/g TOC (average 28 ±18 mg CO_2/g TOC), while sample T8 is considered an

ACCEPTED MANUSCRIPT

outlier with a value of 90 mg CO_2/g TOC. The PP index shows values between 12.87 and 221.52 mg HC/g rock (average 102 ± 63.53 mg HC/g rock).

The dysodile-like samples show S1 values ranging between 0.04 and 2.47 mg HC/g rock (average 1.06 ± 0.92 mg HC/g rock), S2 values between 0.97 and 158.45 mg HC/g rock (average 73.6 ± 58.09 mg HC/g rock) and S3 values between 0.76 and 11.12 mg CO_2/g rock (average 5.02 ± 3.57 mg CO_2/g rock). The TOC values of the dysodile-like samples vary between 2.5 and 38% (average 18.81 ± 12.07%), while the TIC values are between 0.16 and 1.01% (average 0.58 ± 0.26%), and the Tmax values range from 416 to 438 ˚C (average 429 ± 6 ˚C). The boxplot considers sample RAH2 as an outlier, having a Tmax of 402 ˚C. This low Tmax could be due to the presence of amber in this sample. The calculated HI ranges from 30 to 675 mg HC/g TOC (average 340 ± 182 mg HC/g TOC), while OI varies from 7 to 46 mg CO_2/g TOC (average 30 ± 12 mg CO_2/g TOC) and the PP from 1.01 to 159.53 mg HC/g rock (average 74.7 ± 58.85 mg HC/g rock).

The non-dysodiles are characterized by S1 values between 0.05 and 5.41 mg HC/g rock (average 0.90 ± 1.48 mg HC/g rock), S2 values between 3.68 and 59.63 mg HC/g rock (average 19.00 ± 15.37 mg HC/g rock), and S3 values between 2.17 and 24.62 mg CO_2/g rock (average 8.64 ± 6.69 mg CO_2/g rock). TOC values range from 3 to 35% (average 12.87 ± 9.30%), TIC values from 0.17 to 1.09% (average 0.61 ± 0.28%), and Tmax from 396 to 435 ˚C (average 424 ± 10 ˚C). HI values are between 77 and 203 mg HC/g TOC (average 145 ± 42 mg HC/g TOC), OI values between 24 and 116 mg CO_2/g TOC (average 61 ± 26 mg CO_2/g TOC) and PP values between 3.96 and 60.06 mg HC/g rock (average 19.58 ± 15.72 mg HC/g rock). For this group of rocks, many outliers were identified, corresponding to two samples. Sample Ham has a low Tmax value of 375 ˚C probably due to the presence of amber, and sample RaseM that has a very high TOC (52%), S2 (201.77 mg HC/g rock), HI (388 mg HC/g TOC) and PP (207.18 mg HC/g rock), making it a very special sample.

ACCEPTED MANUSCRIPT

Accordingly, by comparing the averages of each parameter, the dysodile shales have higher S1, S2, TIC, HI and PP values, lower S3 and OI values, while Tmax is almost the same for the 3 facies, and TOC is always higher than 10 but slightly higher for the dysodile-like samples.

5.2. Elemental analysis

The elemental analysis results on the isolated organic matter (table 4) indicate high concentrations of carbon for the dysodile samples, varying between 50 and 77 wt.% (average 65.6 ± 6.8 wt.%). These values are coupled with a hydrogen content varying between 3.5 and 8.9 wt.% (average 7.5 ± 1.3 wt.%), and oxygen content ranging from 4.8 to 14.5 wt.% (average 9.4 ± 2.8 wt.%). The corresponding percentage of nitrogen is low, with values between 0 and 1.7 wt.% (average 1.1 ± 0.4 wt.%), while the percentage of sulfur is variable between 0.6 and 12 wt.% (average 3.4 ± 3.2 wt.%). It should be noted that the organic matter concentrates are devoid of carbonates and silicates, but still contain iron dioxides (pyrite and marcasite), leading to high sulfur values.

The dysodiles-like samples are also characterized by high amounts of carbon (average 64.9 ± 9.8 wt.%), hydrogen content varying between 5 and 7.5 wt.% (average 6.4 ± 0.9 wt.%) and oxygen content ranging from 6 to 11.6 wt.% (average 9.6 ± 1.7 wt.%). The nitrogen and sulfur concentrations are always low, respectively between 0.4 and 1.3 wt.% (average 0.9 ± 0.3 wt.%) for N and between 0.6 and 1.2 wt.% (average 1.0 ± 0.2 wt.%) for S with the exception of one sample containing up to 11 wt.% of sulfur.

Considering the non-dysodiles, the percentage of carbon varies between 56 and 74 wt.% (average 66.5 ± 6.1 wt.%), while the percentage of hydrogen varies between 4 and 7 wt.% (average 5.3 ± 1.0 wt.%) and the oxygen is relatively high ranging from 9 to 14 wt.% (average 11.7 ± 1.7 wt.%). The nitrogen content is low, with values between 0.5 and 3 wt.%

ACCEPTED MANUSCRIPT

(average 1.3 ± 0.8 wt.%), but the sulfur content is higher than in the other two groups, varying from 0.5 to 4.6 wt.% (average 2.5 ± 1.6 wt.%), with the exception of one sample having 13 wt.% of sulfur.

On an elemental scale, a clear differentiation of the three facies is not possible. Nevertheless, a slight difference is that non-dysodiles have less hydrogen, and more oxygen.

In accordance with the above data, for the dysodiles H/C ratios vary between 1.2 and 1.6 (average 1.4 ± 0.2) with the exception of one sample (0.73) and O/C between 0.06 and 0.19 (average 0.1 ± 0.04). For the dysodiles-like samples, H/C is between 1.08 and 1.42 (average 1.2 ± 0.1) and O/C between 0.09 and 0.16 (average 0.1 ± 0.03). Finally, the non-dysodiles have low H/C varying between 0.84 and 1.14 (average 1 ± 0.1), and O/C varying between 0.10 and 0.16 (average 0.1 ± 0.02).

5.3. Palynofacies analysis

Table 5 gives the results of palynofacies analysis. The amorphous organic matter (AOM) prevails in all of the investigated samples. This component constitutes between 86 and 99% (average 95 ± 3%) of the total organic matter extracted from the dysodile shales, between 67 and 95% (average 84 ± 11%) of the total organic matter extracted from the dysodile-like samples and between 52 and 93% (average 69 ± 15%) of the total organic matter extracted from the non-dysodiles. It is important to mention that one dysodile-like sample (Tan1) containing 67% of AOM, has 26% of organic components belonging to Botryococcus colonies (fresh water algae).

Phytoclasts are present with variable amounts in the three rock types. They show a percentage of 1 to 10 (average 4 ± 2%) in the dysodile shales, 5 to 24 (average 10 ± 7%) in the dysodile-like samples and 7 to 47 (average 30 ± 15 %) in the non-dysodiles.

ACCEPTED MANUSCRIPT

In comparison (fig. 5), the total organic matter isolated from the dysodile samples contains the highest amounts of AOM, and the lowest amounts of phytoclasts, while the non-dysodiles are characterized by the lowest amounts of AOM and the highest amounts of phytoclasts.

The AOM found in the dysodile samples shows strong fluorescence, while the AOM found in the dysodile-like samples has only weak fluorescence, and the AOM forming the non-dysodiles shows almost no fluorescence (fig.6).

5.4. Organic petrography

Petrographic analysis reveals a difference in the maceral composition of the dysodiles, dysodile-like samples, and non-dysodiles. The polished dysodile sections perpendicular to bedding show a dominance of liptinite macerals, specifically lamalginite forming a fluorescent matrix in the Barremian (fig.7, Qr6 & T5) and Albian samples (fig.7, BM2). Some cutinite (Cu) and vitrinite macerals (Vr) were also identified as well as pyrite (fig.7). The dysodile-like sections show more diversified macerals, including Botryococcus colonies (fig.7, Tan1) and liptinite such as larger cutinite, and sporinite macerals (Sp). The non-dysodile sections also contain liptinite macerals, including a lot of sporinite and cutinite, as well as inertinite macerals.

Vitrinite reflectance (VRr) values measured on all 31 samples are presented in table 6. All studied samples show low VRr varying between 0.25 and 0.43% for dysodile samples (average 0.32%), between 0.27 and 0.48% for dysodile-like (average 0.39%), and 0.46 % for non-dysodiles with the exception of only one sample having VRr of 0.60%. These values are in general accordance with the observed low Tmax values.

5.5. Molecular geochemistry

The molecular analysis focuses only on the aliphatic hydrocarbons fraction, since all samples are clearly immature.

ACCEPTED MANUSCRIPT

While looking at the dysodiles chromatograms (fig.8), we can see three main distributions for the aliphatic compounds: 1. Samples with a dominance of short-chained *n*-alkanes (*n*-C_{12} – *n*-C_{20}); 2. Samples with a dominance of long-chained *n*-alkanes (*n*-C_{28} – *n*-C_{35}); 3. Samples where both, short-chained and long-chained *n*-alkanes occur.

Chromatograms of the dysodiles-like samples reveal two different distributions, either with a dominance of long-chained *n*-alkanes (similar to the dysodiles samples), or with *n*-alkanes distributed over the full range of detection, but with a general decrease in concentration towards the long-chained *n*-alkanes.

The chromatograms of the non-dysodiles exhibit a distribution of n-alkanes over the full range (*n*-C_{12} – *n*-C_{35}).

Table 7 summarizes calculated ratios of molecular compounds for the three rock types. Dysodile samples have Pr/Ph ratios between 0.5 and 6 with an average of 2.6, Pr/*n*-C_{17} ratios between 0.86 and 31.58 (average 5.9) and Ph/*n*-C_{18} ratis ranging from 1.1 to 13.6 (average 4.7). The terrigenous to aquatic ratio (TAR), calculated according to the formula $TAR = \frac{(nC_{27}+nC_{29}+nC_{31})}{(nC_{15}+nC_{17}+nC_{19})}$ (Bourbonniere and Meyers, 1996), has values between 0.17 and 10.5 (average 3.1), and the carbon preference index (CPI) calculated using the formula: $CPI = 2 * \frac{(nC_{23}+nC_{25}+nC_{27}+nC_{29})}{(nC_{22}+2*(nC_{24}+nC_{26}+nC_{28})+nC_{30})}$ (Bray and Evans, 1961) between 0.17 and 4.47 (average 2).

Dysodiles-like samples have Pr/Ph ratios between 5.4 and 8 (average 6), Pr/*n*-C_{17} ratios between 1 and 7 (average 3.1) and Ph/*n*-C_{18} ratios between 0.1 and 3.7 (average 1.2). The calculated ratios TAR and CPI, respectively, vary between 0.74 and 5.87 (average 3) and 1.16 and 2.31 (average 2).

The Pr/Ph ratios for the non-dysodiles vary between 4 and 8.5 (average 6.4), Pr/*n*-C_{17} between 1.8 and 15.4 (average 8.6), and Ph/*n*-C_{18} ratios between 0.3 and 4.4 (average 2.4).

ACCEPTED MANUSCRIPT

TAR has a minimum of 0.56 and a maximum of 4.89 (average 2.7), while CPI has a minimum of 0.6 and a maximum of 2.36 (average 1.5).

6. Discussion

Origin of the Organic matter

High TOC levels reaching up to 50% may be the result of the high primary productivity and/or of the excellent preservation of the OM due to anoxic bottom water conditions (Demaison and Moore, 1980; Baudin *et al*., 2017). To study the origin of this OM, we use the pseudo-van Krevelen diagram (fig.9). It indicates that the dysodile shales and the dysodiles-like shales contain hydrogen-rich type I – II kerogen, mainly derived from algal (phytoplankton) organic matter. In contrast, non-dysodiles contain to a type III organic matter either derived from terrestrial or strongly degraded algal organic matter (Horsfield *et al*., 1994).

Furthermore, Botryococcus colonies observed both in the palynofacies analysis and in the polished sections reveal that the organic matter in some dysodiles-like samples derives from fresh water algae (Rippen *et al*., 2013; Pickel *et al*., 2017). Besides, the petrographic analysis clearly shows the predominance of liptinite macerals, specifically alginite in the dysodile samples, proving the algal origin of the OM (Pickel *et al*., 2017).

A higher terrestrial input is obvious in the dysodile-like and especially in the non-dysodile samples, where phytoclasts (deriving from ligno-cellulosic plant debris; Tyson, 1995), cutinite (formed from cuticules of leaves and stems), and sporinite (deriving from spores and pollen grains) are present in important amounts.

Since the dominance of short-chained *n*-alkanes in the range of 15 to 19 carbon atoms indicates algal/phytoplankton-derived OM (Cranwell *et al.*, 1987; Peters *et al*., 2005), long-chained *n*-alkanes in the range of 25 to 31 carbon atoms indicate terrestrial OM, often

ACCEPTED MANUSCRIPT

accompanied by a strong bacterial component (Peters *et al*., 2005). The geochemical data indicate a larger algal/phytoplankton component in the dysodiles as compared to the other two sample sets.

TAR values are quite fluctuating and indicate a variable terrestrial input from sample to another. Usually values <1 result from the dominance of algal and planktonic OM over terrestrial OM, while values >1 manifest the dominance of terrestrial OM (Peters *et al*., 2005). For the dysodiles-like and non-dysodiles, we see an accordance between the TAR and the abundance of phytoclasts. Nevertheless, a problem is clear for the dysodiles samples, since the partly high TAR corresponds to samples with a low percentage of phytoclasts and fluorescent AOM, meaning that there is no other evidence of terrestrial OM, neither in the palynological samples nor in the organic petrology data. In addition, elemental composition and Rock-Eval data do not support a major terrestrial input. This could be due to the contribution of some non-marine algae to the C_{27} and C_{31} *n*-alkanes, causing the increase of TAR (Moldowan *et al*., 1985; Derenne *et al*., 1988).

Pr/Ph ratios indicate anoxic conditions when lower than one (Peters *et al*., 2005), which is consistent with the high TOC and the preservation of the organic matter. However, we can clearly see that this ratio is much higher for most of the samples. This fact might be explained by the presence of sources of pristane other than chlorophyll, such as zooplankton or bacterial lipids (Ten Haven et al., 1987). This can cause an increase in the Pr/Ph ratio and thus give erroneously an indication of an oxic environment (Peters *et al*., 2005). This explanation might be plausible for the samples, where presence of bacterial OM is highly probable (mainly dysodiles samples).

The Pr/*n*-C_{17} vs Ph/n-C_{18} diagram (fig.10) unravels mainly a mixed origin of the studied OM, with a more terrestrial trend for the dysodiles-like samples and non-dysodiles. This terrestrial

ACCEPTED MANUSCRIPT

input is in agreement with the high phytoclast content and non-fluorescent AOM. Yet, the effect of the biodegradation is quite relevant; it is easier for the bacteria to attack the *n*-alkanes than the isoprenoids, causing Pr/*n*-C_{17} and Ph/*n*-C_{18} to increase; thus the sample shifts towards the upper right corner of the diagram (Peters *et al*., 1999). However, Pr/*n*-C_{17} vs Ph/*n*-C_{18} should be treated with cautions, since it is not giving enough information on its own. Further molecular interpretations should be done in order to understand the trend this diagram is giving.

Petroleum potential and maturity

Before discussing the petroleum potential of these organic-rich facies, it is important to recall their limited lateral extension and metric thickness onshore Lebanon.

Since a high TOC content is coupled with a high S2, and a PP (S1+S2) > 6 mg HC/g rock for most samples, we can consider these organic-rich rocks as very good and excellent source rocks (Peters, 1986).

The HI-OI diagram (fig.9) indicates that the dysodiles and the dysodiles-like samples both contain an oil prone type I to type II kerogen, while non-dysodiles contain a type III gas prone kerogen (Espitalié *et al*., 1977) having high OI and low HI values. The palynofacies and the macerals observed microscopically support these results. The fluorescence of the AOM is in accordance with the high HI, and the dysodiles are richest in lamalginite and liptinites in general.

All the geochemical and petrographical maturity parameters demonstrate that all samples are thermally immature, but probably reached a burial depth between several 100 meters (minimum) and about 1500 – 2000 m (maximum). Low Tmax values (Espitalié *et al*., 1984) coupled with low vitrinite reflectance (<0.5%) show that these organic-rich rocks did not

ACCEPTED MANUSCRIPT

reach the oil window. In addition, the high fluorescence is consistent with the thermal immaturity of all samples.

Likewise, the van Krevelen diagram (fig.11) supports the previous results, not only revealing the type of kerogen, but also showing that all of the samples are still immature and in their early diagenesis stage.

Nevertheless, thermal maturity is controlled by burial depth. In Lebanon, the Bekaa valley is considered as a synclinal structure filled with thick Tertiary and Quaternary sediments (average 2900 m) (Nader et *al*., 2016). Cross-sections and seismic interpretations show that the Upper Jurassic, the Lower Barremian and the Albian are represented in the Bekaa valley at a maximum depth between – 3000 m and – 4000 m (Nader et *al*., 2016). If the dysodiles and associated facies are also deposited there, it is probable that they have reached thermal maturity and have generated their oil. Additionally, since a Jurassic – Lower Cretaceous petroleum system is expected along the Levant Basin margin (Bou Daher *et al.*, 2016), where sufficient maturity is reached, the dysodiles, dysodiles-like shales and non-dysodiles could act as secondary source rocks generating hydrocarbons that would accumulate in the Upper Jurassic carbonate and Lower Cretaceous sandstones reservoirs.

Comparison with other local and regional source rocks

Our study demonstrates the presence of organic-rich deposits in the Kimmeridgian, Lower Barremian and Albian stages onshore Lebanon. Table 8 compares dysodiles, dysodiles-like samples and non-dysodiles to other potential source rocks studied by Bou Daher *et al*. (2014, 2015 and 2016). According to their work, the potential source rocks onshore Lebanon belong to a type II, type IIS and a type III kerogen.

Compared to the other immature Lebanese source rocks, dysodiles have higher TOC, S2 and HI, and lower OI values. This is also valid for the dysodiles-like shales and even for non-

ACCEPTED MANUSCRIPT

dysodiles of the Lower Barremian. Meanwhile, dysodiles-like samples of the Kimmeridgian have lower TOC, S2 and OI, and a higher HI than the Kimmeridgian shales described by Bou Daher *et al*. (2016). This is normal since the source-rock described by Bou Daher *et al*. (2016) is of type III kerogen while the dysodiles-like are of type I to II making them a better source-rock. However, the non-dysodiles from the Kimmeridgian have a lower TOC, S2, HI and a higher OI. When comparing the herein presented source rocks to the previously studied ones, we should keep in mind the small thickness and limited lateral extension of the dysodiles, dysodiles-like shales and non-dysodiles deposits.

Thus, one major remaining question is related to the regional distribution of these lacustrine source rocks, both in the offshore and onshore area. The most important source rocks described in the southern and eastern Tethyan regions are mainly marine shales (Shaaban *et al*., 2006; Kendall *et al*., 2014), containing type II to III kerogen. Fluvio-deltaic sequences including lacustrine deposits are however, also known and might have significant petroleum potential. For example, such rocks are encountered in the Lower Cretaceous (i.e., Lebanese Sandstone (Grès du Liban) unit in Lebanon; Palmyra/ Rutbah Sandstone in Syria; Kurnub Sandstone in Israel and Jordan; Nubian Sandstone in Libya; Zubair Formation in Iraq and Kuwait). Since the depositional environment of the Kimmeridgian and Albian carbonates are quite different in the region, it is more pertinent to compare the dysodiles of the Lower Barremian to the possible source rocks within the Lower Cretaceous Sandstone unit. In fact, these sandstones are widespread on the Arabian plate and are thought to derive from the erosion of Carboniferous and Permian sandstones (Nader, 2014a); figure 12 shows the regional distribution. We chose to use the paleogeographic map of the Aptian, although the Lower Cretaceous sandstones even if present in the entire region were not deposited at the same time. Nevertheless, the most important part of these sandstones had already been deposited by the Aptian time. The Kurnub group of Jordan is described as a clastic group that

ACCEPTED MANUSCRIPT

contains some small shale deposits of limited extension and thickness (Amireh and Abed, 1999). The Rutbah Formation and Palmyra sandstones of Syria have similarities to the "Grès du Liban", being composed of sandstone, volcanic deposits and shale beds (Caron and Mouty, 2007). In Libya, the Nubian Sandstones of Triassic – Lower Cretaceous age, are considered as a secondary source rock (Hassan and Kendall, 2014). The facies in this region resembles that of the Lower Barremian of Lebanon since there is an alternation of lacustrine mudstones, sandstones, volcanic rocks and thin organic-rich deposits (Ambrose, 2000) containing to a type I oil-prone kerogen (Burwood *et al*., 2003). According to their study, Triassic lacustrine shales have a TOC of 4.8%, S2 of 29.7 mg HC/g rock, and an HI of 619 mg HC/g TOC, while the Lower Cretaceous lacustrine shales in the terrestrial unit have a TOC of 2.5%, S2 of 11.2 mg HC/g rock, and an HI of 455 mg HC/g TOC.

In Iraq, few black shale beds crop out in a 64 m thick Triassic fluvial to nearshore marine sandstone deposit. These beds have less than 2% TOC and are believed to be insignificant source rocks (Grabowski, 2014). The Lower Cretaceous of Iraq is dominated by non-marine, fluvial to nearshore sandstones alternating with some black shales. They are immature to mature, contaning gas prone type III kerogen. The average TOC values are low, but can reach a maximum of 6.5% (Al-Ameri *et al*., 2010).

The Barremian and Albian sandstones of Kuwait accommodate finely laminated black shales, holding some small grains of amber, pyrite and plant remains. These shales are believed to be fair to very good source rocks, deriving from an immature to mature type II to III kerogen (Abdullah and Kinghorn, 1996). The Barremian shales have a maximum TOC value of 3.1%, a maximum S2 of 12.7 mg HC/g rock, and a maximum HI of 410 mg HC/g TOC. In parallel, the Albian shales have similar TOC and HI values, but the S2 can reach up to 42 mg HC/g rock.

ACCEPTED MANUSCRIPT

The dysodiles studied herein show even higher values of TOC, S2 and HI, indicating significant petroleum potential.

7. Conclusion

Through this study, the Lebanese Jurassic and Cretaceous organic-rich dysodiles and associated facies are characterized for the first time using organic petrography, geochemical and molecular analyses. The following conclusions are accordingly made for the investigated dysodiles, dysodiles-like and non-dysodiles organic-rich facies.

1- All studied samples have good to excellent source rock potential and are still thermally immature.
2- Dysodiles and dysodiles-like sediments contain type I to II kerogen, deriving from algal and bacterial organic matter deposited in a lacustrine environment.
3- Non-dysodiles belong to a type III kerogen deriving from terrestrial OM.
4- Molecular analysis shows variability between the three rock types. Whereas, TAR indicates a variable terrestrial input and algal OM, CPI supports the immaturity of these organic-rich samples, and the distribution of *n*-alkanes reflects the OM origin of the dysodiles (algal and/or bacterial), dysodiles-like sediments and non-dysodiles (more evident land plants input).
5- Compared to other potential source-rocks onshore Lebanon, these organic-rich facies seem to be of better quality (higher TOC, S2 and HI). Even if they are of limited extension, dysodiles, dysodiles-like sediments and non-dysodiles have a good to excellent source rock potential and should not be ignored in petroleum system analysis.

ACCEPTED MANUSCRIPT

Acknowledgments

ACCEPTED MANUSCRIPT

The authors express their gratitude to the “Société Murex” and the Lebanese University for their scholarship grant to L. EL HAJJ. This paper is a contribution to the project “Dysodiles of the Lower Cretaceous of Lebanon: stratigraphical, palaeontological and geochemical characterization” financed by the Lebanese University; and to the activity of the Advanced Micropalaeontology, Biodiversity and Evolutionary Research (AMBER) team directed by D. AZAR. The authors gratefully acknowledge Florence SAVIGNAC for her assistance during laboratory analyses at the ISTeP laboratory Paris; Laura ZIEGER & Donka MACHEREY for their valuable help and samples preparation for the petrographic analysis; Anna ALBERS and Alireza BANIASAD for their well appreciated support for the molecular analysis; and Kai A. HANKE who’s doing his master thesis on the dysodiles of Lebanon. D. AZAR would acknowledge the Chinese Academy of Sciences for the support under the CAS President’s International Fellowship Initiative (PIFI). The authors would also like to thank Christian BLANPIED for his precious comments on an earlier draft and Cevat Ozgen KARACAN, Sedat INAN and an anonymous reviewer for their valuable comments and suggestions allowing us to improve the manuscript

References

ABDULLAH, F.H.A., KINGHORN, R.R.F., 1996. A preliminary evaluation of Lower and Middle Cretaceous source rocks in Kuwait. Journal of Petroleum Geology, 19 (4), 461 – 480.

AL-AMERI, T.K., PITMAN, J., NASER, M.E., ZUMBERGE, J., AL-HAYDARI, H.A., 2010. Programmed oil generation of the Zubair Formation, southern Iraq oil fields: results from Petromod software modeling and geochemical analysis. Arabian Journal of Geosciences, 4 (7-8), 1239 – 1259.

AMBROSE G., 2000. The geology and hydrocarbon habitat of the Sarir Sandstone, SE Sirt Basin, Libya. Journal of Petroleum Geology, 23 (2), 165 – 192.

ACCEPTED MANUSCRIPT

AMIREH, B.S., ABED, A.M., 1999. Depositional environments of the Kurnub Group (Early Cretaceous) in northern Jordan. Journal of African Earth Sciences, 29 (3), 449 – 468.

BARRIER, E., VRIELYNCK, B., BROUILLET, J.-F., BRUNET, M.-F., 2018. Map 8 Late Aptian (119 – 113 Ma). Paleotectonic reconstruction of the central tethyan realm. Darius programme.

BAUDIN, F., TRIBOVILLARD, N., TRICHET, J., 2017. Géologie de la matière organique. 2nd Edition. Société géologique de France, Vuibert, Paris, France. 326 pp.

BEHAR, F., BEAUMONT, V., de B. PENTEADO, H.L., 2001. Rock-Eval 6 technology: performances and developments. Oil & Gas Science and Technology - Rev. IFP Energies nouvelles, 56 (2), 111 – 134.

BOHACS, K., CARROLL, A., NEAL, J., MANKIEWICZ, P., 2000. Lake-basin type, source potential, and hydrocarbon character: an integrated-sequence-stratigraphic-geochemical framework. In: GIERLOWSKI-KORDESCH, E.H., KELTS, K.R. (Eds.): Lake basins through space and time. AAPG Stud. Geol., 46, 3 – 34.

BOTTA, P.,1831. Sur la structure géognostique du Liban et de l'Anti-Liban. Bulletin de la Société Géologique de France, 10, 234 – 239.

BOU DAHER, S., NADER, F.H., STRAUSS, H., LITTKE, R., 2014. Depositional environment and source-rock characterization of organic-matter rich Upper Santonian – Upper Campanian carbonates, northern Lebanon. Journal of Petroleum Geology, 37 (1), 5 – 24.

BOU DAHER, S., NADER, F.H., MÜLLER, C., LITTKE, R., 2015. Geochemical and petrographic characterization of Campanian – Lower Maastrichtian calcareous petroleum source rocks of Hasbayya, South Lebanon. Marine and Petroleum Geology, 64, 305 – 323.

ACCEPTED MANUSCRIPT

BOU DAHER, S., DUCROS, M., MICHEL, P., HAWIE N., NADER, F.H., LITTKE, R., 2016. 3D thermal history and maturity modelling of the Levant Basin and its eastern margin, offshore-onshore Lebanon. Arabian Journal of Geosciences, 17, 3161. (doi.org/10.1007/s12517-016-2455-1).

BOURBONNIERE, R.A., MEYERS, P.A., 1996. Sedimentary geolipid records of historical changes in the watershed and productivities of Lake Ontario and Erie. Limnology and Oceanography, 41 (2), 352 – 359.

BRAY, E.E., EVANS, E.D., 1961. Distribution of *n*-paraffins as a clue to recognition of source beds. Geochimica et Cosmochimica Acta, 22 (1), 2 – 15.

BREW, G., BARAZANGI, M., AL-MALEH, A.K., SAWAF, T., 2001. Tectonic and geologic evolution of Syria. GeoArabia, 6 (4), 573 – 616.

BURWOOD, R., REDFERN, J., COPE, M.J., 2003. Geochemical evaluation of East Sirte Basin (Libya) petroleum systems and oil provenance. In: ARTHUR, T.J., MACGREGOR, D.S., CAMERON, N.R. (Eds.): Petroleum geology of Africa: New themes and developing technologies. Geological Society of London, Special Publications, 207, 203 – 240.

CARON, C., MOUTY, M., 2007. Key elements to clarify the 110 million year hiatus in the Mesozoic of eastern Syrian. GeoArabia, 12 (2), 15 – 36.

CARVAJAL-ORTIZ, H., GENTZIS, T., 2015. Critical considerations when assessing hydrocarbon plays using Rock-Eval pyrolysis and organic petrology data : Data quality revisited. International Journal of Coal Geology, 152, 113 – 122.

COMBAZ, A., 1980. Les kérogènes vus au microscope. In: DURAND, B. (Ed.): Kerogen: Insoluble organic matter from sedimentary rocks. Technip, Paris, 55 – 112.

ACCEPTED MANUSCRIPT

CORDIER, L., 1808. Sur le dysodile, nouvelle espèce minérale. Journal des Mines, 23, 271 – 274.

CRANWELL, P.A., EGLINTON, G., ROBINSON, N., 1987. Lipids of aquatic organisms as potential contributors to lacustrine sediments II. Organic Geochemistry, 11 (6), 513 – 527.

DEMAISON, G.J., MOORE, G.T., 1980. Anoxic environments and oil source bed genesis. AAPG Bulletin, 64, 1179 – 1209.

DERENNE, S., LARGEAU, C., CASADEVALL, E., CONNAN, J., 1988. Comparison of torbanites of various origins and evolutionary stages. Bacterial contribution to their formation. Cause of lack of botryococcane in bitumens. Organic Geochemistry, 12, 43 – 59.

DUBERTRET, L., 1934. Premières recherches sur les hydrocarbures minéraux dans les états du Levant sous mandat Français. Annales de l'Office national des combustibles liquides, 10, 877 – 899.

DURAND, B., MONIN, J., 1980. Elemental analysis of kerogens (C, H, O, N, S, Fe). In: DURAND, B. (Ed.): Kerogen: Insoluble organic matter from sedimentary rocks. Technip, Paris, 113 – 142.

DURAND, B., NICAISE, G., 1980. Procedures for kerogen isolation. In: DURAND, B. (Ed.): Kerogen: Insoluble organic matter from sedimentary rocks. Technip, Paris, 35 – 54.

ESPITALIÉ, J., LAPORTE, J.L., MADEC, M., MARQUIS, F., LEPLAT, P., PAULET, J., BOUTEFEU, A., 1977. Méthode rapide de caractérisation des roches mères, de leur potentiel pétrolier et de leur degré d'évolution. Oil & Gas Science and Technology - Rev. IFP Energies nouvelles, 32 (1), 23 – 42.

ESPITALIÉ, J., MARQUIS, F., BARSONY, I., 1984. Geochemical logging. Analytical pyrolysis techniques and applications, 276 – 304.

ACCEPTED MANUSCRIPT

ESPITALIÉ, J., DEROO, G., MARQUIS, F., 1985. La pyrolyse Rock-Eval et ses applications (première partie). Revue de l'Institut Français du Pétrole, 40 (5), 563 – 579.

FEINSTEIN, S., AIZENSHTAT, Z., MILOSLAVSKI, I., GERLING, P., SLAGER, J., McQUILKEN, J., 2002. Genetic characterization of gas shows in the eat Mediterranean offshore of southwestern Israel. Organic Geochemistry, 33 (12), 1401 – 1413.

FRAAS, O., 1878. Geologisches aus dem Libanon. Jahreshefte des Vereins fur vaterlandische Naturkunde, Württemberg, 34, 257 – 391.

GHALAYINI, R., NADER, F.H., BOU DAHER, S., HAWIE, N., CHBAT W.E., 2018. Petroleum systems of Lebanon: an update and review. Journal of Petroleum Geology, 41 (2), 189 – 214.

GRABOWSKI Jr., G.J., 2014. Iraq. In: MARLOW, L., KENDALL, C., YOSE, L. (Eds.): Petroleum systems of the Tethyan region. AAPG memoir, 106, 379 – 467.

GRANIER, B., AZAR, D., MAKSOUD, S., GÈZE, R., HABCHI, R., 2015. New fossiliferous sites with Barremian Charophyta in the "Grès du Liban" auct. (Lebanon), with a critical perspective regarding the nature of Munieria Deecke, 1883. Carnets de Géologie, 15 (15), 199 – 229.

GRANIER, B., TOLAND, C., GÈZE, R., AZAR, D., MAKSOUD, S., 2016. Some steps toward a new story of the Jurassic-Cretaceous transition in Mount Lebanon. Carnets de Géologie, 16 (8), 247 – 269.

HASSAN, H.S., KENDALL, C.C.G., 2014. Hydrocarbon provinces of Libya: A petroleum system study. In: MARLOW, L., KENDALL, C., YOSE, L. (Eds.): Petroleum systems of the Tethyan region. AAPG Memoir, 106, 101 – 141.

ACCEPTED MANUSCRIPT

HORSFIELD, B., CURRY, D.J., BOHACS, K., LITTKE, R., RULLKOTTER, J., SCHENK, H.J., RADKE, M., SCHAEFER, R.G., CARROLL, A.R., ISAKSEN, G., WITTE, E.G., 1994. Organic geochemistry of freshwater and alkaline lacustrine sediments in the Green River Formation of the Washakie Basin, Wyoming, USA. Organic Geochemistry, 22, 415 – 455.

HUNT, J.M., 1995. Petroleum geochemistry and geology. W.H. Freeman and Company, New York, 743 pp.

JANENSCH, W., 1925. Fische aus dem Dysodil des Wealden vom Libanon. Zeitschrift der Deutschen geologischen gesellschaft (Abhandlungen und Monatsberichte), 53 – 59.

KELTS, K., 1988. Environments of deposition of lacustrine petroleum source rocks: An introduction. In: FLEET, A.J., KELTS, K., TALBOT, M.R. (Eds.): Lacustrine petroleum source rocks. Geological society of London, Special Publications, 40, 3 – 26.

KENDALL, C.G.C., ALSHARHAN, A.S., MARLOW, L., 2014. Stratigraphy and depositional systems of the southern Tethyan region. In: MARLOW, L., KENDALL, C., YOSE, L. (Eds.): Petroleum systems of the Tethyan region. AAPG Memoir, 106, 29 – 57.

MOLDOWAN, J.M., SUNDARAMAN, P., SCHOELL, M., 1985. Sensitivity of biomarker properties of depositional environment and/or source input in the Lower Toarcian of SW Germany. Organic Geochemistry, 10, 915 – 926.

NADER, F.H., 2011. The petroleum prospectivity of Lebanon: an overview. Journal of Petroleum Geology, 34, 135 – 136.

NADER, F.H., 2014 a. Insights into the petroleum prospectivity of Lebanon. In: MARLOW, L., KENDALL, C., YOSE, L. (Eds.): Petroleum systems of the Tethyan region. AAPG Memoir, 106, 241 – 278.

ACCEPTED MANUSCRIPT

NADER, F.H., 2014 b. The geology of Lebanon. Scientific Press Ltd., Beaconsfield, UK. 108 pp.

NADER, F.H., BROWNING-STAMP, P., LECOMTE, J.-C., 2016. Geological interpretation of 2D seismic reflection profiles onshore Lebanon: implications for petroleum exploration. Journal of Petroleum Geology, 39 (4), 333 – 356.

NOUJAIM CLARK, G., BOUDAGHER-FADEL, M.K., 2001. The larger benthic foraminifera and stratigraphy of the Upper Jurassic/Lower Cretaceous of Central Lebanon. Revue de Micropaléontologie, 44, 215 – 232.

PETERS, K.E., 1986. Guidelines for evaluating petroleum source rock using programmed pyrolysis. AAPG Bulletin, 70 (3), 318 – 329.

PETERS, K.E., FRASER, T.H., AMRIS, W., RUSTANTO, B., HERMANTO, E., 1999. Geochemistry of crude oils from eastern Indonesia. AAPG Bulletin, 83 (12), 1927 – 1942.

PETERS, K.E., WALTERS, C.C., MOLDOWAN, J.M., 2005. The biomarker guide. In: Biomarkers and isotopes in petroleum exploration and Earth history, second ed., vol. 2. Cambridge University Press, Cambridge, 475 – 1155.

PICKEL, W., KUS, J., FLORES, D., KALAITZIDIS, S., CHRISTANIS, K., CARDOTT, B.J., MISZ-KENNAN, M., RODRIGUES, S., HENTSCHEL, A., HAMOR-VIDO, M., CROSDALE, P., WAGNER, N., ICCP, 2017. Classification of liptinite – ICCP system 1994. International Journal of Coal Geology, 69: 40 – 61.

RIELEY, G., COLLIER, R.J., JONES, D.M., EGLINTON, G., EAKIN, P.A., FALLICK, A.E., 1991. Sources of sedimentary lipids deduced from stable carbon-isotope analyses of individual compounds. Nature, 352, 425 – 427.

ACCEPTED MANUSCRIPT

RIPPEN, D., LITTKE, R., BRUNS, B., MAHLSTEDT, N., 2013. Organic geochemistry and petrography of the Lower Cretaceous Wealden black shales of the Lower Saxony Basin: The transition from lacustrine oil shales to gas shales. Organic geochemistry, 63, 18 – 36.

SACHSE, V.F., LITTKE, R., JABOUR, H., SCHÜMANN T., KLUTH, O., 2012. Late Cretaceous (late Turonian, Coniacian and Santonian) petroleum source rocks as part of an OAE, Tarfaya Basin, Morocco. Marine and Petroleum Geology, 29 (1), 35 – 49.

SHAABAN, F., LUTZ, R., LITTKE, R., BUEKER C., ODISHO, K., 2006. Source-rock evaluation and basin modeling in NE Egypt (NE Nile Delta and northern Sinai). Journal of Petroleum Geology, 29 (2), 103 – 124.

TALBOT, M., ALLEN, P., 1996. Lakes. In: READING, H.G. (Ed.): Sedimentary environments, processes, facies and stratigraphy. Blackwell publishing, UK, 83 – 124.

TEN HAVEN, H.L., de LEEUW, J.W., RULLKÖTTER, J., SINNINGHE DAMASTÉ, J.S., 1987. Restricted utility of the pristane/ phytane ratio as a palaeoenvironmental indicator. Nature, 330, 641 – 643.

TISSOT, B.P., WELTE, D.H., 1984. Petroleum formation and occurrence, Springer-Verlag, New York, 699 pp.

TYSON, R., 1995. Sedimentary organic matter: organic facies and palynofacies. Chapman and Hall, London, 615 pp.

VANDENBROUCKE, M., LARGEAU, C., 2007. Kerogen origin, evolution and structure. Organic Geochemistry, 38, 719 – 833.

VELTZ, I., 2008. Le Passage Jurassique Crétacé au Liban. Thèse de doctorat, Université de Reims Champagne-Ardenne, Reims, France, 279 pp.

ACCEPTED MANUSCRIPT

ZIMMERLE, W., 1985. New aspects on the formation of hydrocarbon source rocks. Geologische Rundschau, 74 (2), 385 – 416.

ACCEPTED MANUSCRIPT

ACCEPTED MANUSCRIPT

Table 1. List of all the sampling sites divided into dysodiles, dysodiles-like and non-dysodiles, with the number of samples used from each site, its age and GPS coordinates. The coordinates are not given to second level in order to protect the sampling sites

Code	Sampling site	Nb of samples	Age	GPS coordinates
		Dysodiles		
JB	Jdaydet Bkessine	3	Lower Barremian	N 33˚33' E 35˚34'
Qr	Qrayn	7	Lower Barremian	N 34˚23' E 36˚1'
S	Snyya	7	Lower Barremian	N 33˚31' E 35˚33'
T	Tarchich	11	Lower Barremian	N 33˚51' E 35˚49'
Z	Zehalta	2	Lower Barremian	N 33˚30' E 35˚32'
BM	Beit Mounzer	2	Albian	N 34˚15' E 35˚54'
OuO	Ouadi Oudine	1	Albian	N 34˚32' E 36˚18'
Q	Qnat	2	Albian	N 34˚15' E 35˚54'
		Dysodiles-like		
AinT	Ain Tourine	2	Kimmeridgian	N 34˚17' E 35˚56'
Bl	Blaouza	2	Kimmeridgian	N 34˚15' E 35˚56'
Eh-Aal	Ehmej-Aalmat	1	Kimmeridgian	N 34˚6' E 35˚46'
Haw	Hawka	1	Kimmeridgian	N 34˚16' E 35˚56'
Tan	Tannourine	1	Kimmeridgian	N 34˚13' E 35˚55'
RAH	Roum-Azour-Homsiyeh	4	Lower Barremian	N 33˚33' E 35˚32'
S	Snyya	2	Lower Barremian	N 33˚31' E 35˚33'
		Non-dysodiles		
BeiM	Beit Mounzer	1	Kimmeridgian	N 34˚15' E 35˚55'
Eh-Man	Ehden-Mantara	1	Kimmeridgian	N 34˚17' E 35˚56'
Gh	Ghineh	1	Kimmeridgian	N 34˚2' E 35˚42'
HadeJ	Hadath el Joubeh	1	Kimmeridgian	N 34˚13' E 35˚55'
Qar-Ya	Qartaba-Yanouh	1	Kimmeridgian	N 34˚5' E 35˚51'
Qnai	Qnaiwer	1	Kimmeridgian	N 34˚16' E 35˚55'
Tan	Tannourine	1	Kimmeridgian	N 34˚13' E 35˚55'
Ham	Hammana	1	Lower Barremian	N 33˚48' E 35˚43'
Mak	Maknouniyeh	1	Lower Barremian	N 33˚31' E 35˚32'
Mey	Meyrouba	1	Lower Barremian	N 34˚01' E 35˚46'
Ram	Ramliyeh	1	Lower Barremian	N 33˚45' E 35˚39'
RaseM	Ras el Matn	1	Lower Barremian	N 33˚50' E 35˚39'
T	Tarchich	3	Lower Barremian	N 33˚51' E 35˚49'

ACCEPTED MANUSCRIPT

Table 2. Number of samples used for each method

Rock type	Number of samples	Rock-Eval Pyrolysis	Elemental analysis	Palynofacies analysis	Organic petrography	Molecular geochemistry
Dysodiles	35	35	16	16	21	15
Dysodiles-like	13	13	5	5	8	4
Non-dysodiles	15	15	5	5	3	2

Table 3. Rock-Eval results for all samples showing values of TOC, TIC, S1, S2, S3, Tmax, HI, OI and PP

Sample	TOC (wt.%)	TIC (wt.%)	S1 (mg HC/g rock)	S2 (mg HC/g rock)	S3 (mg CO_2/g rock)	T_{max} (°C)	HI (mg HC/g TOC)	OI (mg CO_2/g TOC)	PP (mg HC/g rock)
Dysodiles									
JB1	20.67	3.10	1.44	159.87	1.60	434	773	8	161.31
JB2	22.40	3.27	1.55	186.27	1.59	433	832	7	187.82
JB3	18.94	2.99	1.55	147.58	2.90	431	779	15	149.13
Qr1	13.09	3.88	7.75	94.53	4.64	423	722	35	102.28
Qr2	22.80	2.76	15.22	165.57	10.79	424	726	46	180.79
Qr3	21.29	5.46	7.88	160.51	5.24	426	754	25	168.39
Qr4	6.62	4.46	1.08	35.44	2.31	427	535	35	36.52
Qr5	18.19	3.69	13.18	137.86	4.46	427	758	25	151.04
Qr6	15.22	3.00	0.67	97.00	5.81	426	637	38	97.67
Qr7	6.63	3.04	1.28	35.40	2.13	426	534	32	36.68
S1	24.89	0.94	2.08	219.44	2.21	434	882	9	221.52
S2	20.97	1.46	1.11	160.70	9.38	435	766	45	161.81
S3	7.99	3.17	0.16	39.95	2.72	427	500	34	40.11
S4	20.39	0.45	1.41	161.10	3.85	435	790	19	162.51
S5	13.41	1.18	0.81	88.76	5.71	431	662	43	89.57
S6	16.18	3.11	1.18	116.19	6.16	433	718	38	117.37
S7	13.84	2.03	0.90	94.90	6.34	435	687	46	95.80
T1	12.96	0.15	1.01	83.16	1.01	428	642	8	84.17
T2	10.23	0.68	0.41	43.95	1.53	422	430	15	44.36
T3	19.99	0.26	2.06	111.98	3.65	424	560	18	114.04
T4	19.93	0.07	2.40	140.91	1.30	431	707	7	143.31
T5	24.16	0.29	2.96	173.31	1.66	434	717	7	176.27
T6	6.12	0.19	0.12	18.49	5.13	422	302	84	18.61
T7	11.52	0.23	0.31	46.15	8.53	424	401	74	46.46
T8	7.12	0.20	0.21	21.80	6.39	431	306	90	22.01
T9	19.16	0.24	3.27	93.11	4.00	417	486	21	96.38
T10	19.04	0.25	2.79	93.60	3.88	418	492	20	96.39
T11	3.15	9.85	0.33	28.82	0.45	440	915	14	29.15
Z1	22.79	0.91	1.46	200.09	4.31	437	878	19	201.55
Z2	22.31	1.04	1.22	195.96	3.29	438	878	15	197.18
BM1	1.42	8.45	0.22	6.28	0.74	421	422	54	6.50
BM2	4.78	6.55	1.26	33.20	0.46	420	695	10	34.46
OuO	11.67	0.31	0.57	59.41	6.36	425	509	54	59.98
Q1	2.00	6.30	1.01	11.86	0.44	410	593	22	12.87
Q2	3.54	7.34	1.92	25.23	0.69	422	713	19	27.15
Dysodiles-like									
AinT1	15.50	0.39	1.09	57.07	5.23	426	368	34	58.16

ACCEPTED MANUSCRIPT

AinT2	27.17	0.46	2.25	110.31	8.72	421	406	32	112.56
Bl1	25.75	0.68	2.47	146.93	2.26	435	571	9	149.40
Bl2	27.94	0.68	1.79	142.61	4.56	433	510	16	144.40
Eh-Aal	35.87	0.53	1.08	158.45	9.05	435	442	25	159.53
Haw	16.76	0.84	0.50	51.91	6.10	432	310	36	52.41
Tan1	10.84	0.19	0.25	73.17	0.76	438	675	7	73.42
RAH1	3.22	0.16	0.04	0.97	1.05	416	30	33	1.01
RAH2	28.94	0.83	1.63	50.32	11.12	402	174	38	51.95
RAH3	8.80	0.31	0.07	5.83	4.07	426	66	46	5.90
RAH4	38.03	0.54	2.45	145.32	10.00	422	381	26	147.77
S8	2.52	1.01	0.10	5.43	1.00	433	215	44	5.53
S9	3.20	0.90	0.06	8.52	1.34	429	266	42	8.58
				Non-dysodiles					
BeiM	15.89	0.65	0.30	29.66	6.61	427	187	42	29.96
Eh-Man	3.01	0.17	0.05	4.90	2.17	433	163	72	4.95
Gh	10.13	0.50	0.19	7.80	11.74	435	77	116	7.99
HadeJ	6.01	0.25	0.21	11.04	2.99	429	184	50	11.25
Qar-Ya	34.95	0.97	0.43	59.63	19.16	431	170	55	60.06
Qnai	9.18	0.34	0.22	13.84	7.88	428	151	86	14.06
Tan2	16.54	0.50	0.32	33.61	12.24	428	203	74	33.93
Ham	28.06	0.95	3.62	34.86	12.65	375	124	45	38.48
Mak	22.77	1.09	1.12	27.64	24.62	396	121	108	28.76
Mey	9.63	0.83	0.05	7.94	2.35	432	82	24	7.99
Ram	7.21	0.25	0.47	8.46	4.17	425	117	58	8.93
RaseM	52.02	0.95	5.41	201.77	14.19	424	388	27	207.18
T12	7.11	0.62	0.58	13.33	3.27	413	187	46	13.91
T13	4.38	0.56	0.28	3.68	3.02	419	84	69	3.96
T14	5.26	0.47	0.23	9.67	2.47	414	184	47	9.90

ACCEPTED MANUSCRIPT

ACCEPTED MANUSCRIPT

Table 4. Elemental analysis results giving the relative percentage of N, C, H, S & O, and the calculated ratios H/C and O/C

Sample	N (%)	C (%)	H (%)	S (%)	O (%)	Total (%)	H/C	O/C
Dysodiles								
JB2	1.25	64.79	7.73	4.53	7.04	85.34	1.43	0.08
Qr2	1.29	57.34	6.92	0.96	7.82	74.33	1.45	0.10
Qr3	1.65	50.32	5.63	0.71	12.07	70.38	1.34	0.18
Qr4	1.02	62.33	7.19	4.46	12.79	87.89	1.38	0.15
S1	1.18	65.13	8.49	2.30	7.60	84.70	1.56	0.09
S3	0.97	60.15	6.78	9.94	9.91	87.75	1.35	0.12
S4	1.04	70.27	8.76	2.52	11.71	94.30	1.50	0.12
S7	1.20	58.62	3.57	0.67	14.46	78.52	0.73	0.19
T1	1.23	71.63	8.02	4.22	6.95	92.05	1.34	0.07
T5	0.00	74.85	8.82	2.20	6.40	92.27	1.41	0.06
T6	1.37	70.52	6.99	0.61	14.08	93.57	1.19	0.15
T7	1.23	71.58	7.79	2.23	8.67	91.50	1.31	0.09
T11	0.71	63.79	8.38	12.13	4.87	89.88	1.58	0.06
Z1	1.11	64.41	8.25	2.73	7.48	83.98	1.54	0.09
OuO	1.03	66.46	7.96	2.86	11.14	89.45	1.44	0.13
Q	1.64	77.11	8.86	0.79	8.03	96.43	1.38	0.08
Dysodiles-like								
AinT2	0.66	62.67	5.63	1.23	10.74	80.93	1.08	0.13
Bl1	1.29	76.69	7.50	0.60	9.80	95.88	1.17	0.10
Bl2	1.19	75.84	7.01	1.17	9.26	94.47	1.11	0.09
Tan1	0.56	54.97	6.50	1.02	6.64	69.69	1.42	0.09
S9	0.82	54.21	5.18	11.27	11.64	83.12	1.15	0.16
Non-dysodiles								
Tan2	0.98	66.35	5.24	0.52	14.11	87.20	0.95	0.16
Ham	0.81	55.95	3.93	13.25	11.09	85.03	0.84	0.15
Ram	1.14	65.97	4.63	3.32	12.68	87.74	0.84	0.14
RaseM	0.54	74.36	6.23	1.47	11.96	94.56	1.01	0.12
T12	2.90	69.67	6.62	4.61	8.89	92.69	1.14	0.10

ACCEPTED MANUSCRIPT

Table 5. Palynofacies analysis results for all samples, showing the relative percentage of the different components found in the isolated organic matter

	Relative percentage of each component (%)			
Sample	**AOM**	**Phytoclasts**	**Sporomorphs**	**Botryococcus**
		Dysodiles		
JB2	98	2	---	---
Qr2	95	4	<1	---
Qr3	97	3	<1	---
Qr4	96	4	<1	---
S1	95	5	<1	---
S3	86	10	4	---
S4	95	5	---	---
S7	94	4	2	---
T1	96	4	<1	---
T5	94	6	<1	---
T6	94	6	---	---
T7	97	3	---	---
T11	96	4	---	---
Z1	97	3	---	---
OuO	92	7	1	---
Q	99	1	---	---
		Dysodiles-like		
AinT2	94	6	---	---
Bl1	95	5	---	---
Bl2	90	10	---	---
S9	75	24	1	---
Tan1	67	7	---	26
		Non-dysodiles		
Tan2	72	27	<1	---
Ham	76	24	<1	---
Ram	52	47	1	---
RaseM	55	45	<1	---
T12	93	7	<1	---

ACCEPTED MANUSCRIPT

Table 6. Vitrinite reflectance results for all samples, with the corresponding TOC and Tmax values.

Sample	TOC (%)	Tmax (˚C)	VRr%	Standard dev.
Dysodiles				
JB2	22.40	433	0.32	0.04
Qr2	22.80	424	0.25	0.04
Qr3	21.29	426	0.26	0.06
Qr4	6.62	427	0.29	0.05
Qr5	18.19	427	0.28	0.05
Qr6	15.22	426	0.41	0.07
Qr7	6.63	426	0.36	0.05
S1	24.89	434	0.37	0.03
S3	7.99	427	0.31	0.05
S4	20.39	435	0.32	0.03
S7	13.84	435	0.23	0.05
T2	10.23	422	0.43	0.03
T5	24.16	434	0.31	0.05
T8	7.12	431	0.39	0.07
T11	3.15	440	0.28	0.05
Z1	22.79	437	0.29	0.04
Z2	22.31	438	0.26	0.03
BM1	1.42	421	0.30	0.06
BM2	4.78	420	0.39	0.04
Ouo	11.67	425	0.30	0.06
Q2	3.54	422	0.35	0.06
Dysodiles-like				
AinT1	15.50	426	0.45	0.06
AinT2	27.17	421	0.27	0.04
Bl1	25.75	435	0.38	0.04
Bl2	27.94	433	0.40	0.05
Eh-Aal	35.97	435	0.44	0.05
Tan1	10.84	438	0.48	0.02
RAH4	38.03	422	0.38	0.05
S9	3.20	429	0.35	0.05
Non-Dysodiles				
Mak	22.77	396	0.46	0.06
Ram	7.21	425	0.46	0.08
RaseM	52.02	424	0.60	0.05

ACCEPTED MANUSCRIPT

Table 7. List of the ratios calculated from the aliphatic fraction (Pr = Pristane; Ph = Phytane; TAR = Terrigenous/aquatic ratio; CPI = Carbon preference index)

Sample	Age	Pr/Ph	Pr/*n*-C_{17}	Ph/*n*-C_{18}	TAR	CPI
Dysodiles						
JB2	Lower Barremian	2.31	4.88	3.58	4.59	1.74
Qr3	Lower Barremian	0.70	1.86	8.41	0.17	0.17
Qr4	Lower Barremian	0.51	0.39	13.61	0.68	3.90
Qr6	Lower Barremian	5.33	8.63	2.45	1.92	1.25
Qr7	Lower Barremian	0.94	0.86	10.17	1.30	1.85
S1	Lower Barremian	2.19	4.19	2.24	4.38	0.21
S3	Lower Barremian	1.45	4.77	3.85	1.10	2.91
S4	Lower Barremian	2.17	3.57	1.86	3.00	3.64
S7	Lower Barremian	1.63	2.74	1.94	6.02	3.09
T2	Lower Barremian	4.46	5.02	1.46	1.38	0.55
T5	Lower Barremian	2.99	6.36	3.31	3.52	2.17
T8	Lower Barremian	4.95	5.18	1.11	3.66	1.71
T11	Lower Barremian	1.26	3.97	4.03	4.59	1.74
Z2	Lower Barremian	2.47	4.13	1.84	10.50	4.47
BM2	Albian	5.58	31.58	9.94	0.27	0.34
Dysodiles-like						
AinT1	Kimmeridgian	5.43	2.97	0.47	5.87	2.17
Bl2	Kimmeridgian	7.85	1.32	0.34	0.74	1.66
Tan1	Kimmeridgian	8.00	1.00	0.15	0.77	1.70
S9	Lower Barremian	2.65	7.09	3.71	4.74	2.31
Non-dysodiles						
RaseM	Lower Barremian	8.47	1.79	0.33	4.89	2.36
T12	Lower Barremian	4.33	15.44	4.41	0.56	0.60

ACCEPTED MANUSCRIPT

ACCEPTED MANUSCRIPT

Table 8. Comparison between the dysodiles, dysodiles-like and non-dysodiles studied in this paper, and the onshore source-rocks studied in a. Bou Daher *et al*., 2016; b. Bou Daher *et al*., 2015; c. Bou Daher *et al*., 2014

	Age	**Thickness (m)**	**TOC (wt.%)**	**S1 (mg HC/g rock)**	**S2 (mg HC/g rock)**	**HI (mg HC/g TOC)**	**OI (mg CO_2 / g TOC)**	**Tmax (°C)**	**VRr (%)**	**Kerogen type**
Carbonates[a]	Upper Paleocene	30	0.8 (±0.3)	0.1 (±0.02)	3.2 (±1.9)	317 (±126)	163 (±57)	427 (±5)	-	II to III
Marly Limestone[b]	Campanian-Lower Maastrichtian	150	5.4 (±2.9)	1.2 (±2.0)	37.4 (±24.0)	617 (±161)	59 (±54)	418 (±8)	0.36 (±0.04)	IIS
Carbonates + Marls[c]	Upper Santonian-Upper Campanian	150	2.4 (±1.1)	0.2 (±0.1)	12.2 (±6.2)	510 (±43)	67 (±13)	426 (±4)	0.25 – 0.40	II
Carbonates[a]	Cenomanian	3 – 4	1.1 (±0.2)	0.2 (±0.02)	9.1 (±1.6)	865 (±25)	115 (±18)	405	0.41 (±0.01)	III
Carbonates[a]	Albian	-	0.5 (±0.1)	0.03 (±0.02)	0.3 (±0.1)	63 (±21)	294 (±40)	420 (±3.5)	-	III/IV
Dysodiles	Albian	3	4.7 (±3.7)	0.9 (±0.6)	27.2 (±18.7)	586 (±110)	32 (±19)	420 (±5)	0.33 (±0.04)	I to II
Coaly shales[a]	Neocomian	12	17.9 (±18.3)	0.5 (±0.5)	17.3 (±23.5)	91 (±61)	80 (±83)	421 (±6)	0.54 (±0.10)	III
Dysodiles	Lower Barremian	3	16.1 (±6.2)	2.6 (±3.6)	111.7 (±58.7)	659 (±166)	30 (±22)	430 (±6)	0.31 (±0.06)	I to II
Dysodiles-like	Lower Barremian	1	14.1 (±14.1)	0.7 (±0.9)	36.1 (±51.6)	189 (±118)	38 (±7)	421 (±10)	0.40 (±0.06)	I to II
Non-dysodiles	Lower Barremian	1	17.1 (±15.5)	1.5 (±1.8)	38.4 (±62.6)	161 (±93)	53 (±25)	412 (±17)	0.51 (±0.06)	III
Shales[a]	Kimmeridgian	0.5	53.3	2.61	158.41	297	31	400	-	III
Dysodiles	Kimmeridgi	1	22.8	1.3	105.8	469	22	431	0.38	I to II

ACCEPTED MANUSCRIPT

-like	an		(±8.1)	(±0.8)	(±41.8)	(±116)	(±11)	(±5)	(±0.07)	
Non-dysodiles	Kimmeridgian	1	13.7 (±9.8)	0.2 (±0.1)	22.9 (±18.1)	162 (±38)	71 (±23)	430 (±3)	-	III

ACCEPTED MANUSCRIPT

ACCEPTED MANUSCRIPT

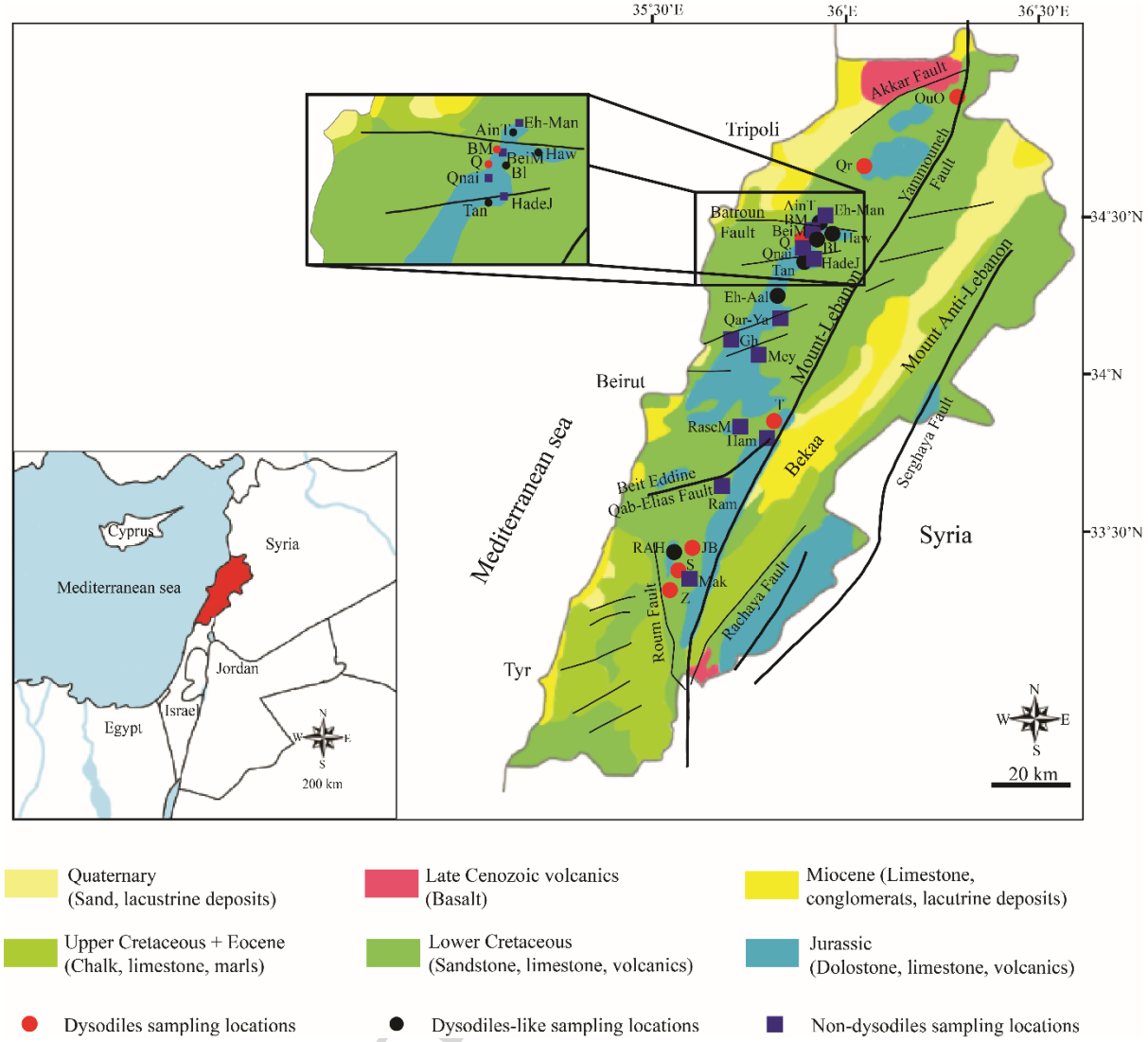

Figure 1. Geological map of Lebanon showing the location of the different sampling sites. Modified from Nader, 2014b

ACCEPTED MANUSCRIPT

ACCEPTED MANUSCRIPT

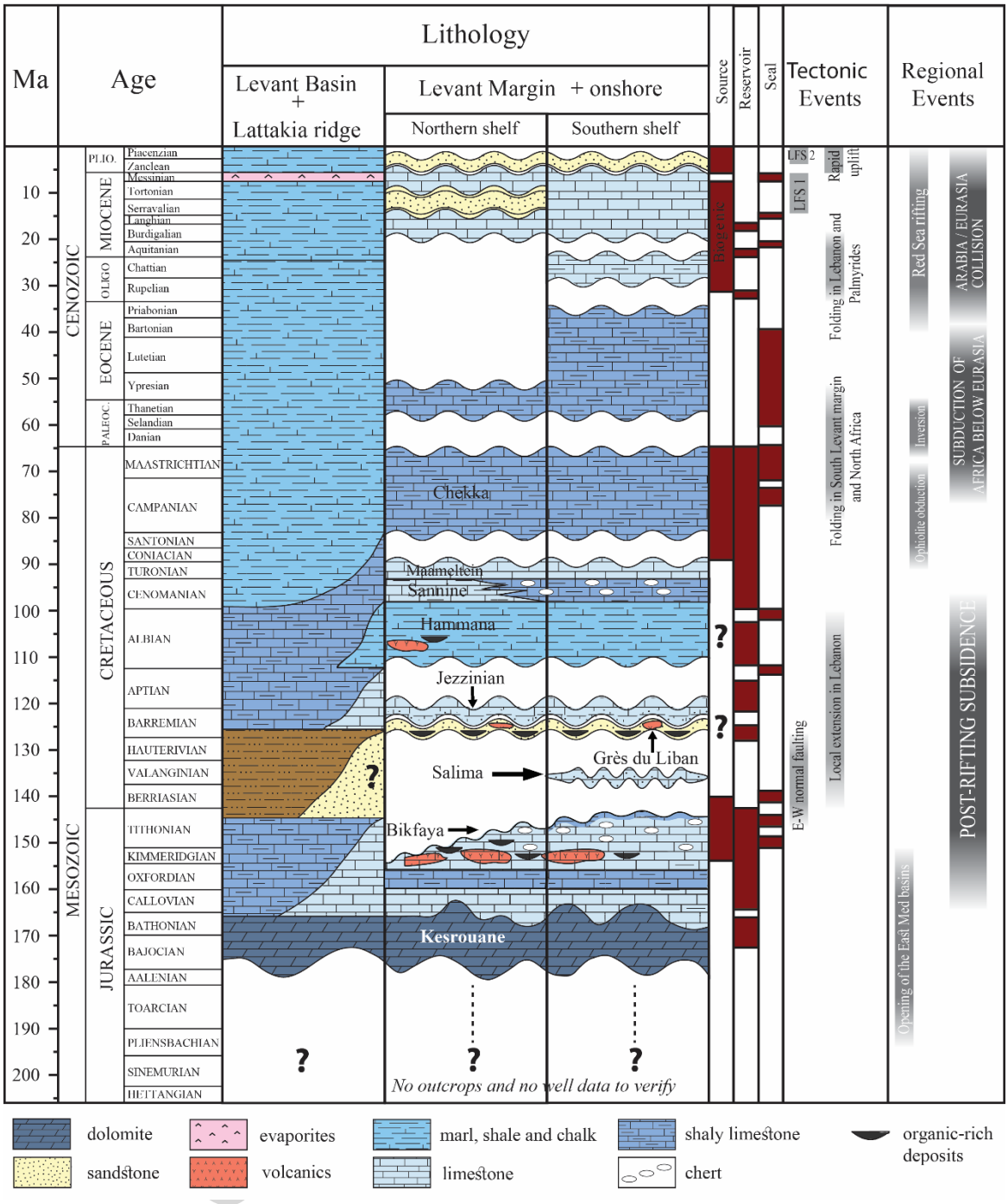

Figure 2. Chronostratigraphic chart showing the sedimentary successions, the major geological events, source rocks, reservoirs and seals found in the Levant Basin, the Levant Margin and onshore Lebanon. Modified from Ghalayini *et al*., 2018

ACCEPTED MANUSCRIPT

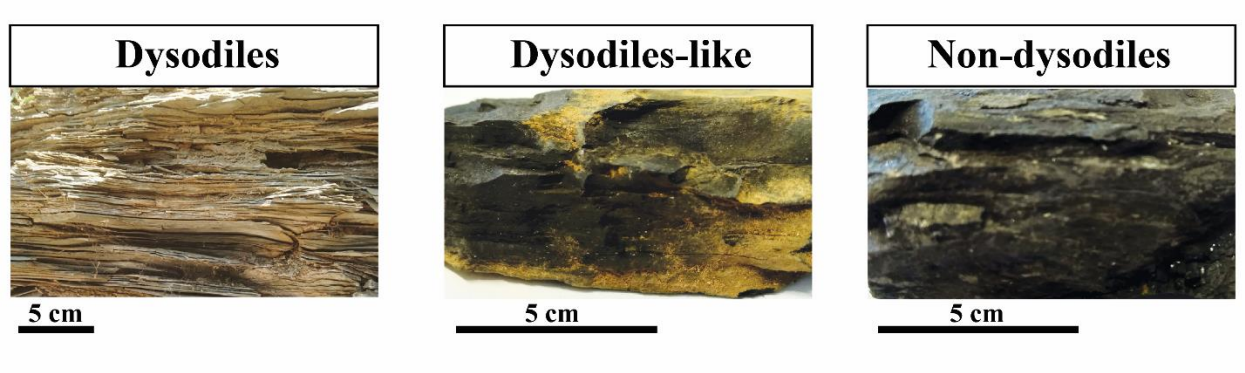

Figure 3. Representation of the dysodiles deposits (sampling site), dysodiles-like and non-dysodiles samples

ACCEPTED MANUSCRIPT

ACCEPTED MANUSCRIPT

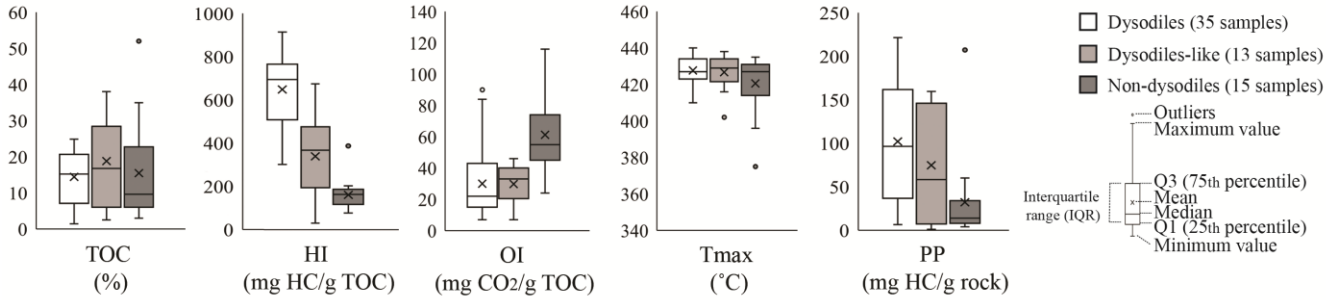

Figure 4. Boxplot showing the range of variation and the outliers of the Rock-Eval results for the three facies. A value is considered as an outlier if it exceeds a distance of 1.5*IQR below Q1 or above Q3

ACCEPTED MANUSCRIPT

ACCEPTED MANUSCRIPT

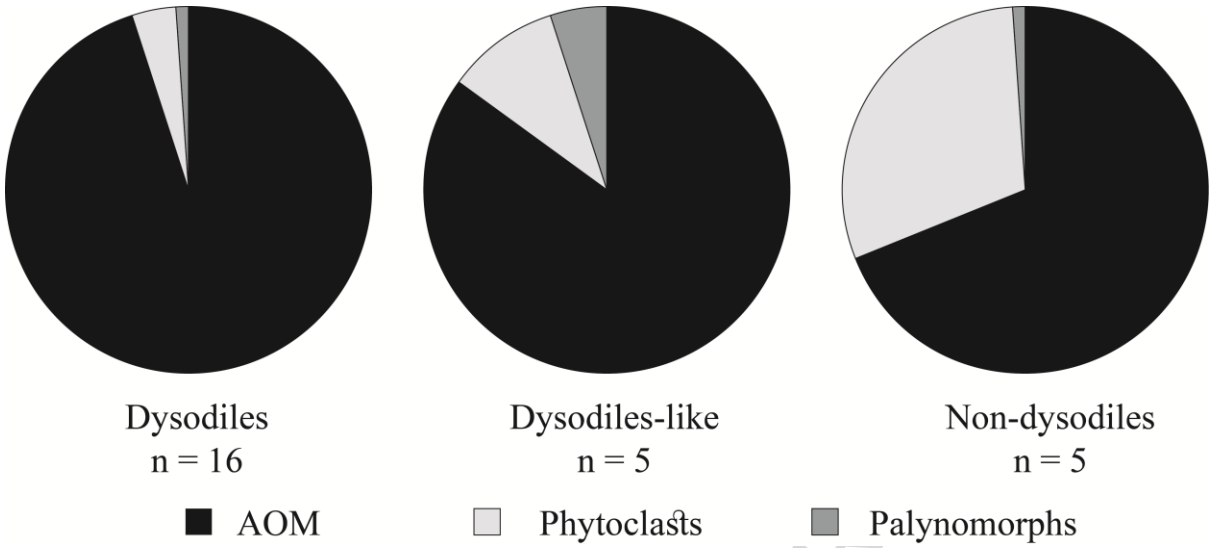

Figure 5. Pie charts illustrating the palynofacies results for dysodiles, dysodiles-like and non-dysodiles (average percentage of each component). It is clear that the dysodiles are richer in AOM, while the non-dysodiles are richer in phytoclasts

ACCEPTED MANUSCRIPT

ACCEPTED MANUSCRIPT

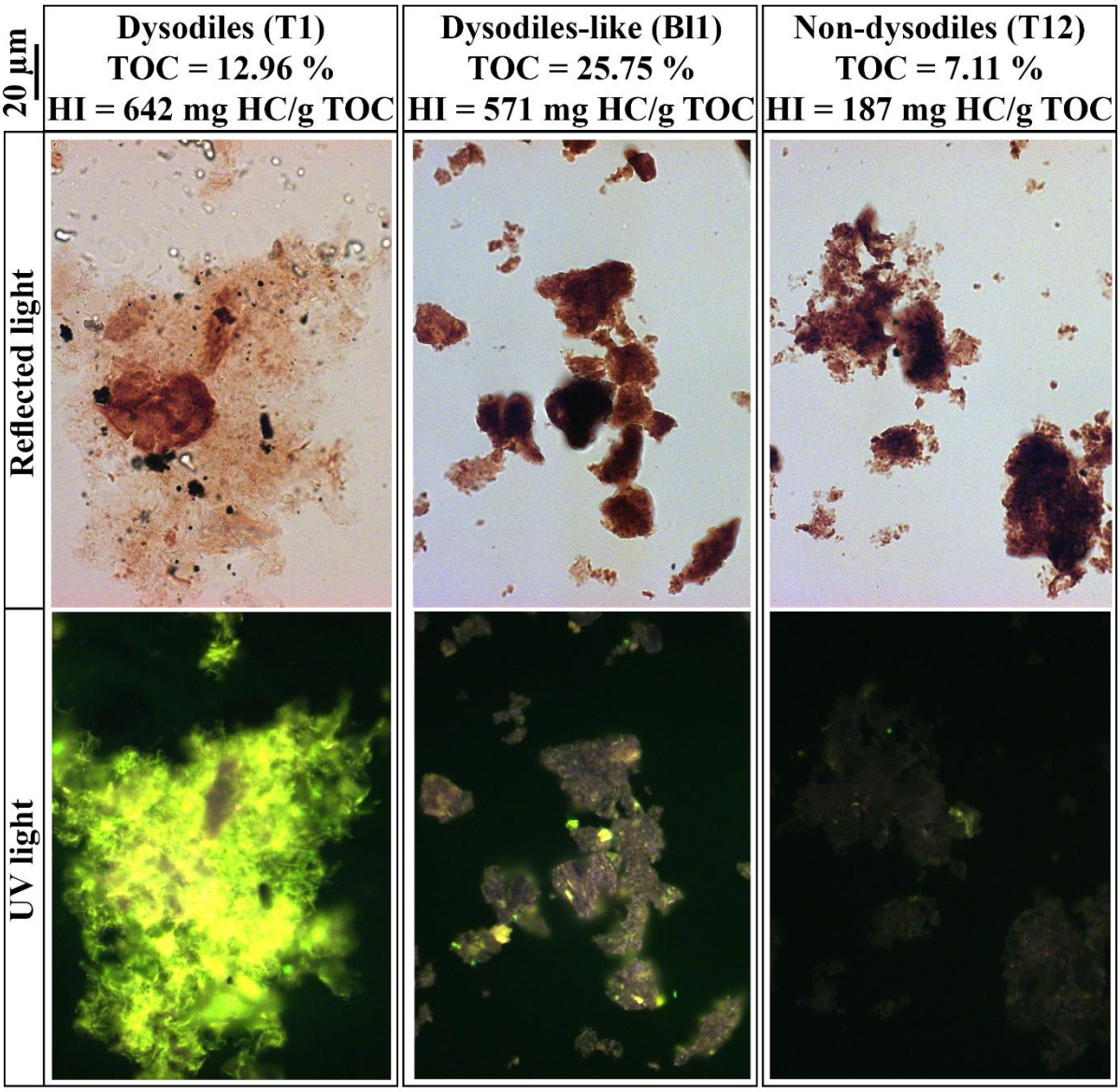

Figure 6. The amorphous organic matter (AOM) observed under reflected and UV light for the dysodiles, dysodiles-like and non-dysodiles. It is clear that the AOM from the dysodile samples is quite fluorescent, while the AOM from the non-dysodiles does not fluoresce

ACCEPTED MANUSCRIPT

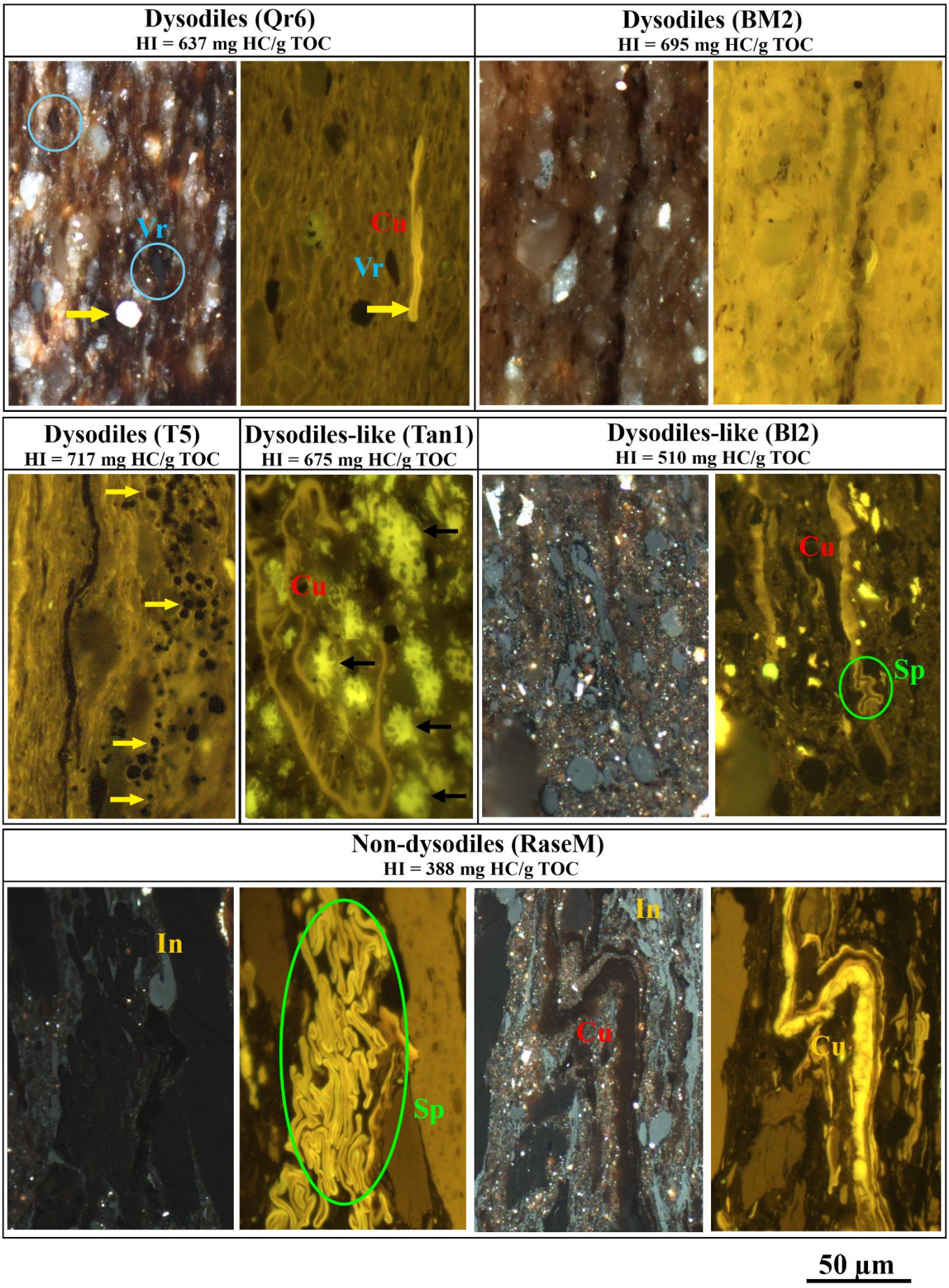

ACCEPTED MANUSCRIPT

Figure 7. Polished sections observed under reflected and UV light. Qr6 is a dysodile from the Lower Barremian showing a matrix of liptinitte containing some vitrinite macerals (Vr), fluorescent cutinite (Cu) and pyrite (yellow arrows). BM2 is a dysodile from the Albian, where the liptinite matrix contains more minerals. T5 is a dysodile from the Lower Barremian containing lots of pyrite (yellow arrows). Tan1 is a polished section of dysodiles-like showing Botryococcus colonies (black arrows) which are freshwater algae. Bl2 is a dysodiles-like showing cutinite (Cu) and sporinite (Sp), deriving from terrestrial organic matter. RaseM is a non-dysodiles richer in sporinite and contains thicker cutinite and inertinite macerals (In), as a proof of an important terrestrial organic matter input

ACCEPTED MANUSCRIPT

ACCEPTED MANUSCRIPT

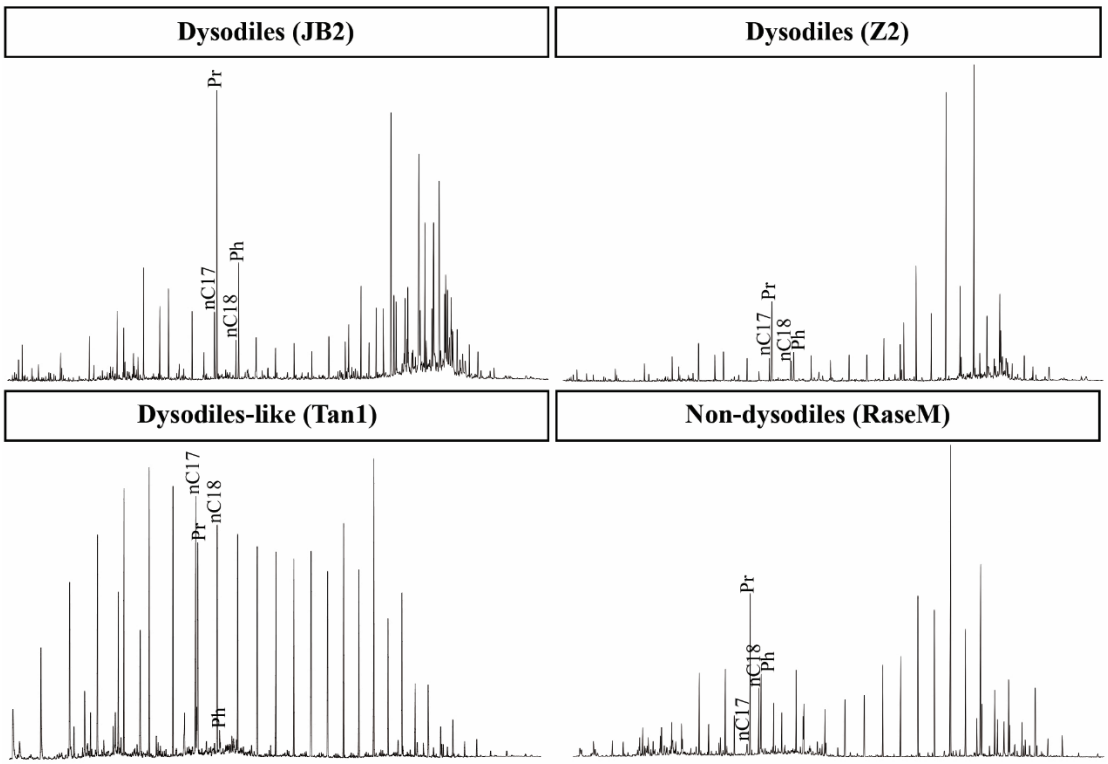

Figure 8. Different representative chromatograms showing two aliphatic compounds distributions for the dysodiles (1) dominance of short-chained and long-chained *n*-alkanes, (2) dominance of long-chained *n*-alkanes; a distribution over the full range of detection for the dysodiles-like and non-dysodiles

ACCEPTED MANUSCRIPT

ACCEPTED MANUSCRIPT

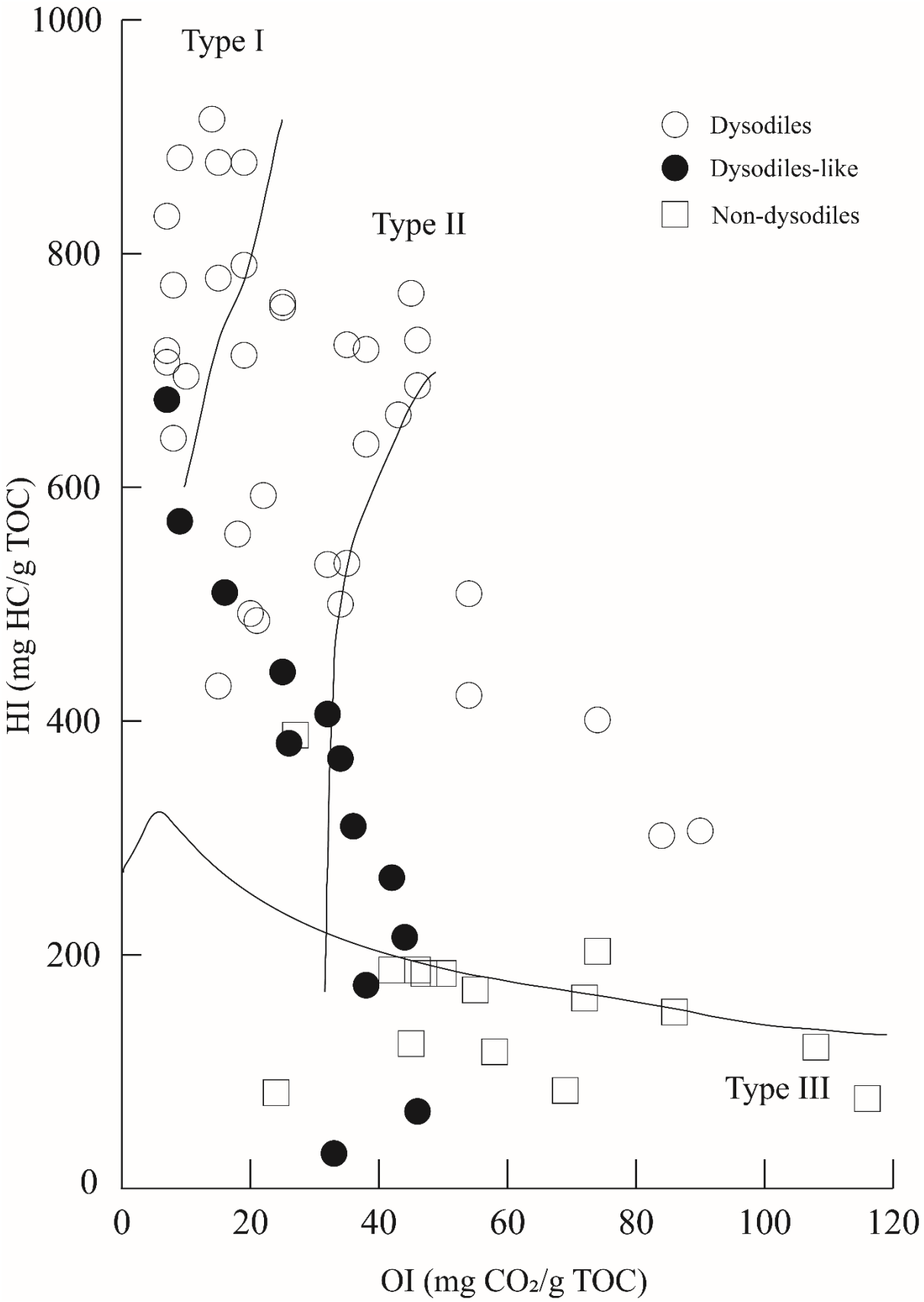

ACCEPTED MANUSCRIPT

Figure 9. HI-OI Pseudo van Krevelen diagram showing that dysodiles and dysodiles-like follow two oxidation trends for a type I-II kerogen, while the non-dysodiles belong to a type III kerogen. Based on Espitalié *et al*., 1985

ACCEPTED MANUSCRIPT

ACCEPTED MANUSCRIPT

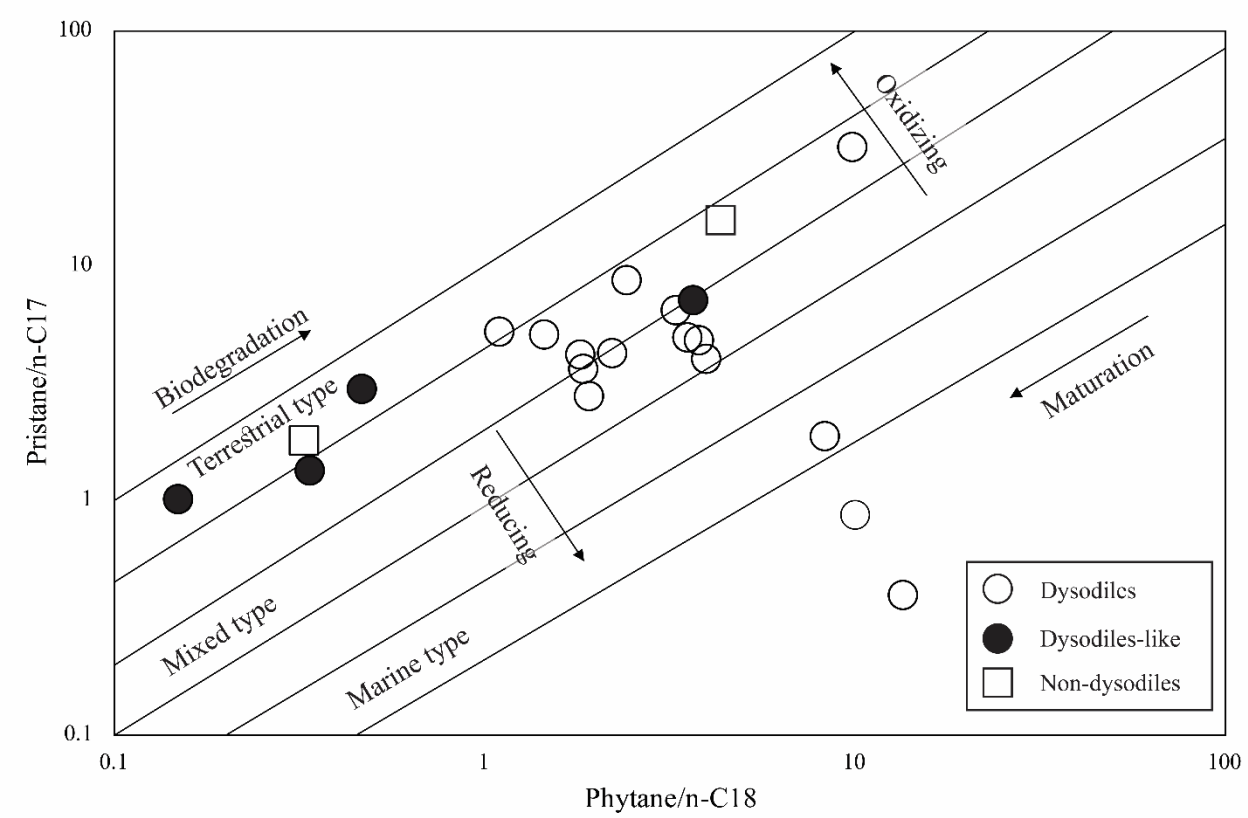

Figure 10. Pristane/*n*-C17 vs Phytane/*n*-C18 diagram studying the organic matter and the depositional environment characteristics. Based on Hunt, 1995

ACCEPTED MANUSCRIPT

ACCEPTED MANUSCRIPT

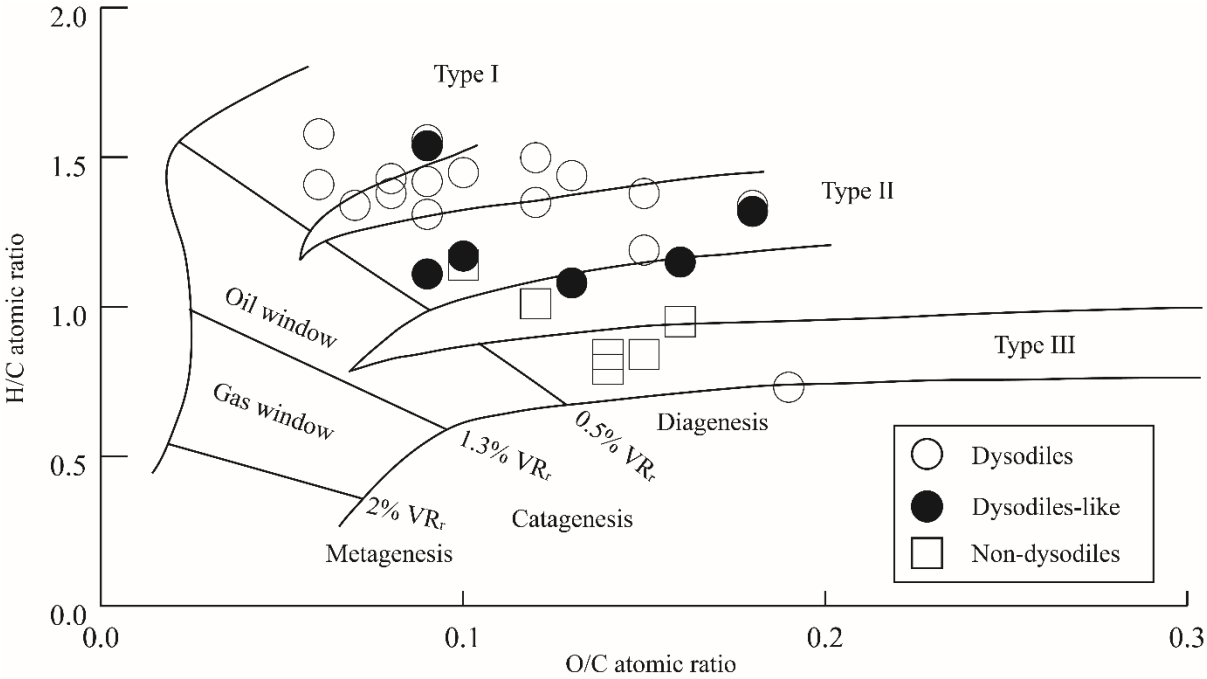

Figure 11. van Krevelen diagram obtained by plotting the results of the elemental analysis, showing the type and maturity of the studied samples. Based on Durand and Monin, 1980

ACCEPTED MANUSCRIPT

ACCEPTED MANUSCRIPT

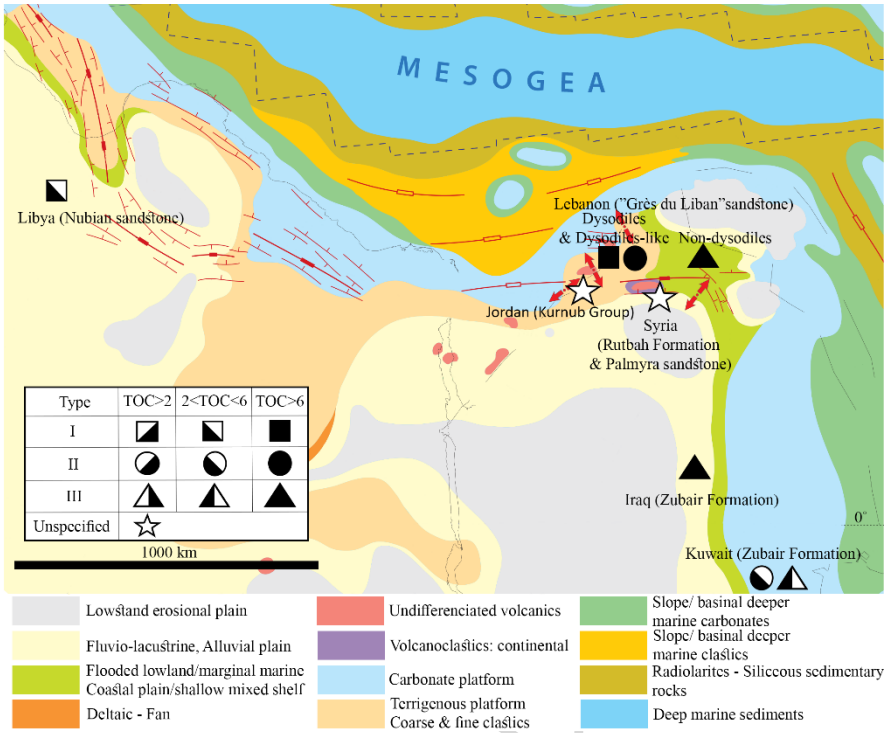

Figure 12. Paleogeographic map of the Tethyan region during the Aptian age, when most of the source rocks compared to the dysodiles in the discussion part, have been deposited. The map shows the regional distribution and characteristics of these source rocks. Modified from Barrier *et al.*, 2018

ACCEPTED MANUSCRIPT

ACCEPTED MANUSCRIPT

Highlights

- New study of organic-rich facies from the Kimmeridgian to the Albian of Lebanon
- Three organic-rich facies are characterized: dysodiles, dysodiles-like & non-dysodiles
- The first 2 facies contain type I-II kerogen, the third contains type III kerogen
- All three facies have excellent source rock potential and are thermally immature

ACCEPTED MANUSCRIPT